To the Graduate Council:

I am submitting herewith a thesis written by William Bruce DeShetler entitled "Feasibility of a Reflective Pressure Transducer." I have examined the final copy of this thesis for form and content and recommend that it be accepted in partial fulfillment of the requirements for the degree of Master of Science, with a major in Electrical Engineering.

Roy D Joseph

Roy D. Joseph, Major Professor

We have read this thesis and recommend its acceptance:

James W. Cunning

Bruce W. Bomar

Accepted for the Council:

Cewminkel

Vice Provost
and Dean of The Graduate School

STATEMENT OF PERMISSION TO USE

In presenting this thesis in partial fulfillment of the requirements for a Master's degree at the University of Tennessee, Knoxville, I agree that the library shall make it available to borrowers under the rules of the library. Brief quotations from this thesis are allowable without special permission, provided that accurate acknowledgement of the source is made.

Permission for extensive quotation from or reproduction of this thesis may be granted by my major professor, or in his absence, by the Head of Interlibrary Services when, in the opinion of either, the proposed use of the material is for scholarly purposes. Any copying or use of the material in this thesis for financial gain shall not be allowed without my written permission.

Signature William B. DeSmith

Date August 1988

FEASIBILITY OF A REFLECTIVE PRESSURE TRANSDUCER

A Thesis

Presented for the

Master of Science

Degree

The University of Tennessee, Knoxville

William Bruce DeShetler

August 1988

ABSTRACT

Most commercial pressure transducers make use of rather mature technologies for converting pressure into more easily manipulated electrical signals. The strain gauge and the capacitive transducer are but two of the more popular methods now in use. This study looks at the feasibility of designing a transducer which measures the amount of light reflected off a diaphragm. This design, termed optical reflective, involves fiber-optics to transmit and collect the light and uses a microprocessor to interpret the raw data.

This thesis considers the complete design of a pressure transducer using the optical reflective technique. Attention is focused in the components' governing equations, with the design emphasis on minimizing the transducer errors. An error analysis is included to indicate the cause and significance of the system uncertainties. Finally, comparisons are made with a large collection of commercial transducers.

With the optical reflective technique a pressure transducer can be designed that has increased accuracy, greater dynamic range, and better temperature stability than is available with today's commercial transducers. The accuracy of this design is better than 0.031% Full Scale, while the higher natural frequency (about double)

permits its use over a larger dynamic range. The temperature dependence is greatly reduced by having the optical circuit completely isolated from the pressure sensing element, thereby eliminating the need for thermal compensation of the electronic circuit.

TABLE OF CONTENTS

LIST OF FIGURES

LIST OF SYMBOLS

A. Physical Constants or Abbreviations.

%FS	per cent of full scale
Hz	Hertz
in.	inch or inches
msec	seconds x 10^{-3}
nm	meters x 10^{-9}
psi	pounds per square inch
V	Volts
μm	meters x 10^{-6}
μsec	seconds x 10^{-6}
μW	Watts x 10^{-6}

B. Diaphragm related symbols and constants

A	Stiffness coefficient in diaphragm deflection equation
a_1	Linear coefficient in diaphragm deflection equation
a_3	Cubic term in diaphragm deflection equation
b	Radius of the diaphragm rigid center
B	Stiffness coefficient in diaphragm deflection equation
b/r_d	Solidity ratio used in determining A and B
E	Modulus of elasticity (psi)
f_n	Fundamental frequency of a diaphragm (Hz)
h	Diaphragm thickness (in.)
P	Pressure difference (psi)
r_d	Diaphragm radius (in.)
μ	Poisson's ratio
W	Specific weight (lb/in.^{3})
y	Deflection distance of the rigid center (in.)
y_{max}	Maximum allowable deflection distance (in.)

C. Optical Sensor symbols and constants

a	Amount of growth in the irradiated light spot due to the N.A. and the distance d (in.)
C_0-C_6	Sixth order polynomial coefficients
d	Distance of the fibers from the diaphragm surface (in.)
N.A.	Numerical Aperture
n_0	Index of refraction of air
n_1	Index of refraction of fiber core
n_2	Index of refraction of fiber cladding
r	Radius of the transmit and receive fiber cores (in.)

R	Radius of the reflected light spot at the fiber (in.)
z	a/r
β_m	Maximum exit angle of flux from fiber
Φ_R	Received light flux (μW)
Φ_T	Transmitted light flux (μW)
Ω	Φ_R/Φ_T

D. Filter and Processor Symbols and Constants

A_{max}	Maximum allowable passband attenuation (dB)
A_{min}	Minimum stopband attenuation (dB)
C	Capacitor or capacitance value
dB	Decibels
G	1/R
H(jw)	H(s) where s=jw, a complex frequency
H(s)	Complex transfer function
K	Gain constant
n	Filter order
R	Resistor or resistance value
S	1/C
V_i	Input voltage signal to the filter
V_o	Output voltage from filter
w	Frequency (rad/sec)
w_c	Cutoff or 3dB frequency

CHAPTER I

INTRODUCTION

A General Information

Research and development in aeropropulsion systems are critical to the success of any modern aerospace vehicle. Aerospace structure and turbine engine testing occur in small test cells where environmental conditions are carefully modeled to simulate actual flight conditions. The ability to effectively model the environment and to understand the behavior of turbine engines or wind tunnel models is closely linked to the ability to accurately measure various parameters near the test articles. Pressure is an important parameter in turbine engines and in aerospace vehicles. The pressures throughout turbine engines are related to the airflows and have to be known and predictable in order to insure proper operation. Likewise, the behavior of the airflow about aerospace vehicles must be known to understand the operating characteristics.

Engine testing and wind tunnel testing both require accurate pressure measurements. Engine test cells measure as many as 600 pressures throughout the engine, while wind tunnels measure more than 200. A large family of pressure transducers has evolved to meet the need of these research and development efforts.

A pressure transducer converts pressure into another physical quantity, usually an electrical output[1]. A pressure transducer consists of two main components, a sensor and a converter. The sensor is usually a diaphragm, a stiff plate which deflects under pressure. The converter is a circuit which converts the diaphragm deflection into an output, usually an electrical signal proportional to the pressure applied. Standard techniques used in today's transducer include resistive strain gauges and capacitive transducers.

As materials and electronics technologies have progressed, pressure transducers have become more reliable and accurate. A promising refinement in transducer technology is the incorporation of optical techniques into transducer design. Groups are already studying interferometric methods for pressure measurements[2]. A transducer design using optical techniques can be expected to produce improved accuracy, frequency characteristics, and temperature dependence.

This thesis looks at the theoretical design of a pressure transducer using optical techniques with microprocessor processing. The optical technique suggested in this study will be referred to as the reflective technique. The reflective technique uses variations in light intensity as a function of distance from a reflective surface. Comparisons to commercial transducers will be made to determine if such a design is suitable for further development.

B General Design

All pressure transducers have certain basic components. Each has a sensor, a device which responds to a differential pressure in a known fashion. In most cases, the sensor is a diaphragm, a metal or semiconductor plate which deflects according to the laws of elasticity under applied pressure (Fig. 1). All transducers have a converter which takes the sensor deflection and converts it to an output which can be easily read, stored, processed, and/or transmitted. Most commercial transducers use electrical outputs for which a nearly linear voltage/pressure relationship exists.

The optical design of this study includes the following items (Fig. 2):

1. A diaphragm designed to be used with the optical method chosen.
2. A fiber optic sensor using the reflective properties of light to measure the distance the diaphragm has deflected.
3. A low pass filter/amplifier to remove the high frequency oscillations produced by the diaphragm.
4. A microprocessor circuit to convert the

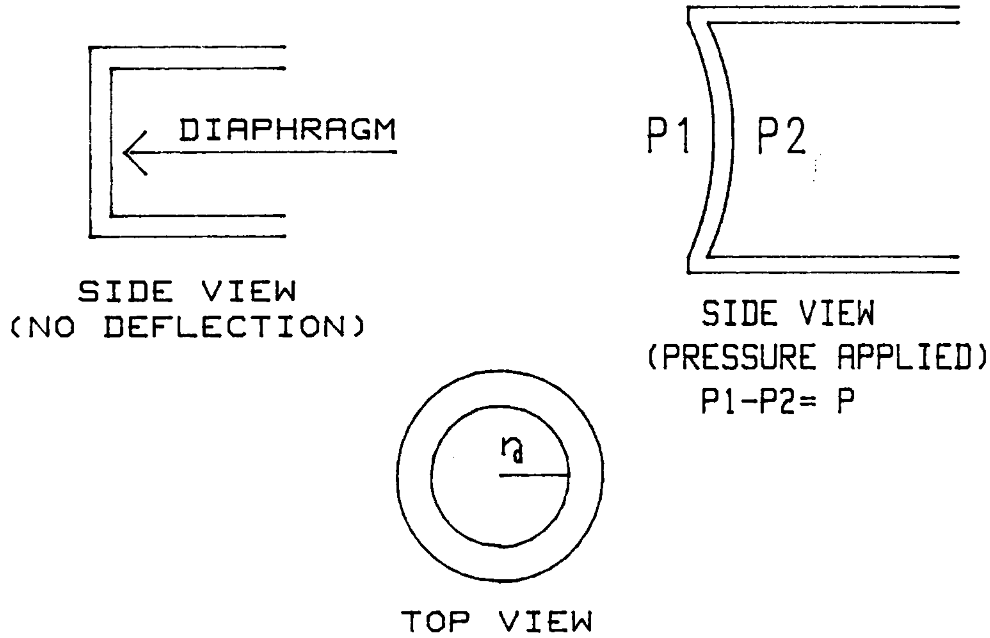

Figure 1: Pressure Diaphragm

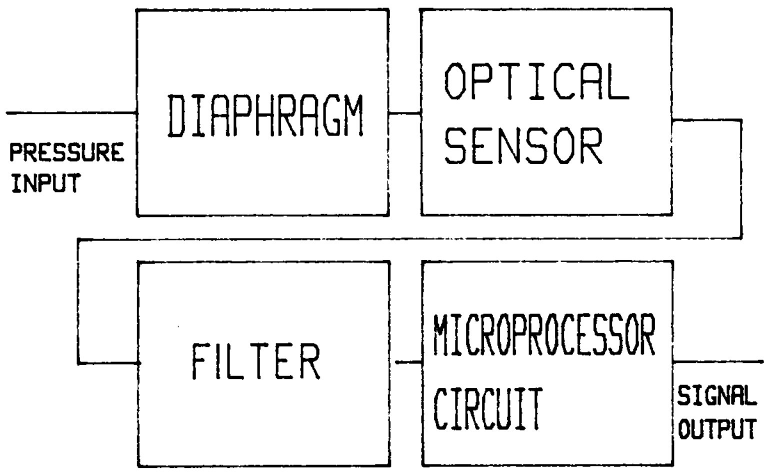

Figure 2: Block Diagram, Optical Pressure Transducer

fiber optic output into an output linearly related to pressure. This also contains an analog to digital converter.

The diaphragm is designed using standard techniques[3]. There are several variables to select in diaphragm design. Consideration must be given to the desired maximum deflection of the diaphragm, the maximum pressure to be measured, the material of the diaphragm, the transducer's environment, the frequency and transient response desired, and other constraints which the designer may impose. The difficult chore in diaphragm design is to optimize the variables so that all the requirements are met.

The optical sensor consists of a light source, a transmitting fiber, receiving fibers, and an optical receiver. The idea of a reflective sensor is to transmit light down a fiber, allow the light to exit the fiber near a reflective surface, and have receiving fibers detect the reflected light (Fig. 3). As the light exits the transmit fiber and is reflected off the diaphragm, the size of the irradiated spot at the receive fibers is proportional to the distance d the fibers are from the diaphragm. The relationship between the size of the irradiated light spot and the distance d is governed by the Numerical Aperture of the fiber used[4]. The amount of light detected by the

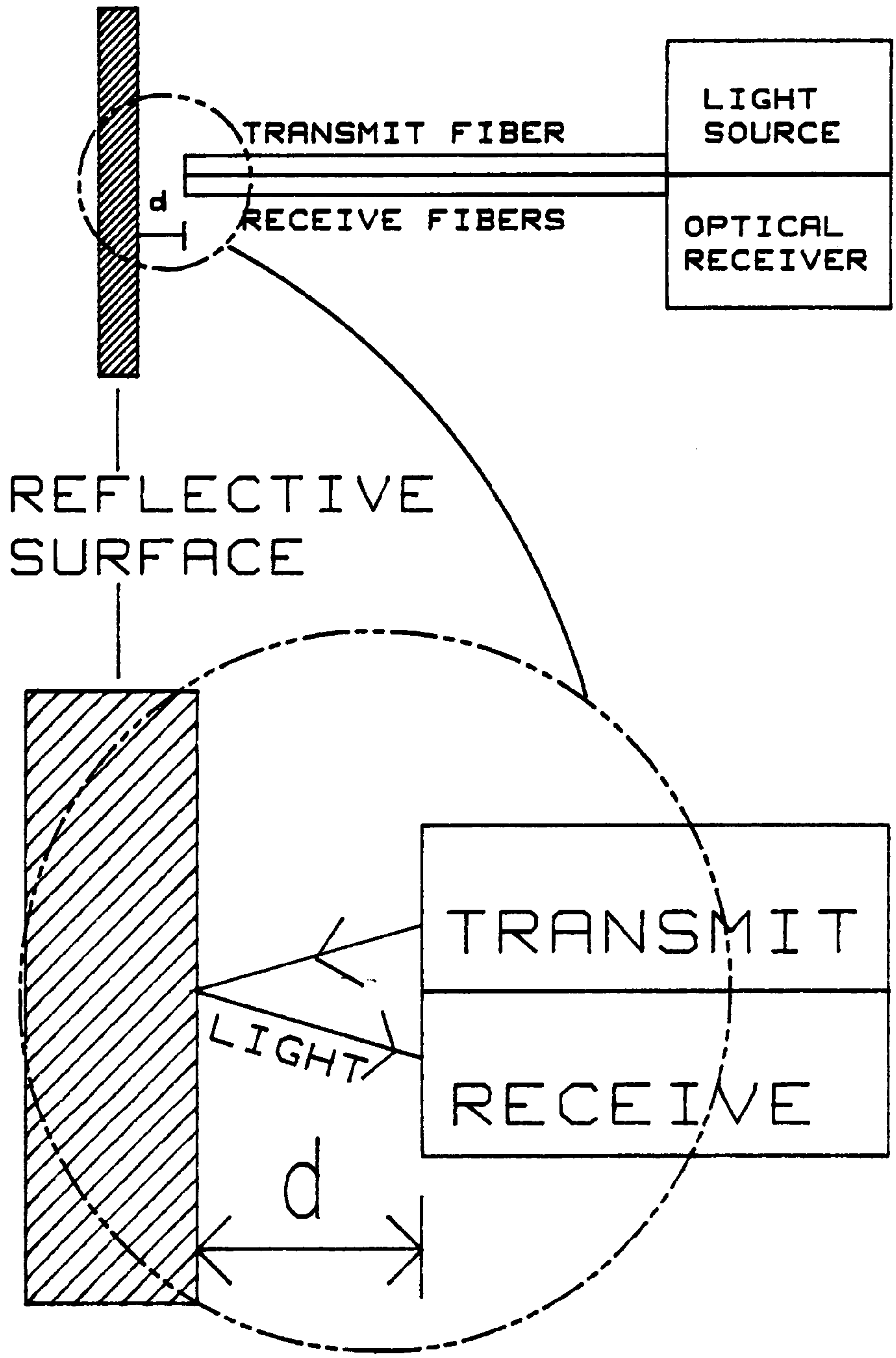

Figure 3: Optical Sensor

receiver is directly related to the distance from the reflecting surface.

The low pass filter/amplifier takes the signal from the optical receiver and amplifies it for better resolution. It also eliminates the high frequency oscillation that the diaphragm experiences, improving the response of the transducer.

The microprocessor circuit consists of an analog to digital (A/D) converter which converts the filter output voltage to a digital form for the microprocessor to process. The microprocessor converts the digital input into a digital output linearly dependent on the pressure. The microprocessor could also be used to control the transducer and has potential for future use as a signal processor.

This study will specifically investigate a 0-50 psi transducer. However, the design method is valid over a wide range of transducer pressures.

CHAPTER II

DETAILED DESIGN

A Diaphragm Design

1. Theory of Operation

Diaphragms are flexible plates which undergo elastic deflection under pressure[5]. Extensive research has been carried out on diaphragms since they are important in many types of instrumentation.

For use as a pressure measuring device, the diaphragm is inserted into the air flow (Fig. 1). If the pressures P1 and P2 are not equal, the diaphragm deflects towards the side of least pressure. The amount of deflection that the diaphragm undergoes is proportional to the pressure difference, P1-P2. Pressures can be applied until the pressure difference becomes so great that the elastic limit is exceeded and the diaphragm is permanently deformed[6].

A circular diaphragm design will be used in this study. Circular diaphragms are universally used because of their simplicity of design and their linear behavior under small deflections[7].

The circular diaphragm's characteristic equation is of the form

$$P = a_1 y + a_3 y^3 \qquad (1)$$

where P is the applied pressure difference, y is the deflection distance of the centerpoint, and a_1 and a_3 are constants determined by the material and dimensions of the diaphragm[8].

For the reflective transducer, a circular diaphragm with a rigid center has been chosen. The rigid center allows the use of the diaphragm as a reflective surface for measuring the distance the diaphragm has moved.

A flat diaphragm with a rigid center has a center which is much thicker than the rest of the diaphragm (Fig. 4). The thickness of the rigid center must be at least six times the diaphragm thickness in order to be effective[9]. The radius of the rigid center is defined as b, and the radius of the diaphragm is r_d. The ratio b/r_d is called the solidity ratio. The coefficients a_1 and a_3 in the characteristic equation for the diaphragm depend on b/r_d.

2. Assumptions and Equations

Diaphragm design and theory is based on the following assumptions[10]:

1. Each surface of the diaphragm is flat and of uniform thickness. For the rigid center diaphragm, the rigid center and the thinner, elastic portion of the diaphragm are assumed to be of uniform thickness.

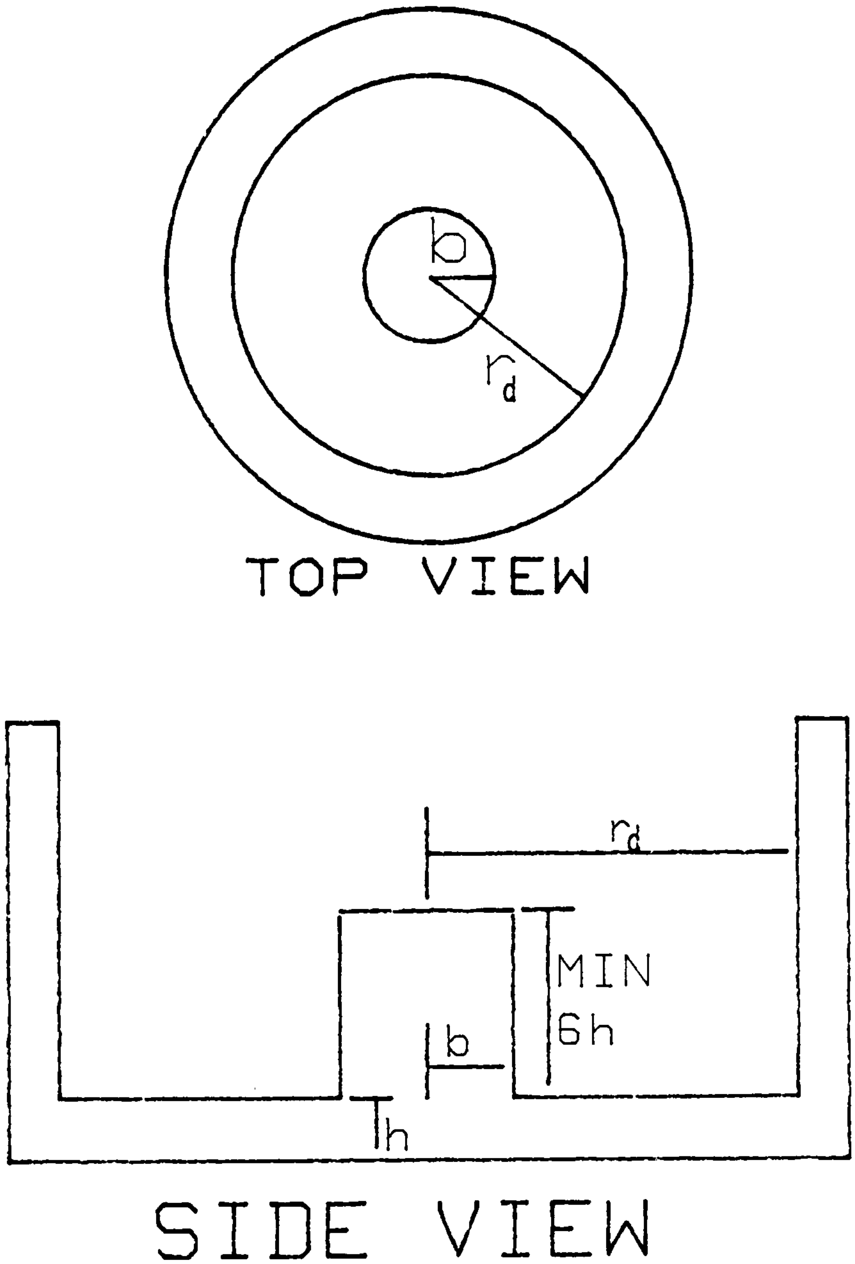

Figure 4: Flat Diaphragm with Rigid Center

2. The material is isotropic and homogeneous.
3. The maximum deflection does not exceed 30% of the thickness of the plate.
4. All forces are applied normal to the plate.
5. The plate is not stressed beyond the elastic limit.
6. The plate's thickness is not greater than 20% of the diameter.

The list of assumptions is not restrictive since all of the conditions are easily met. The governing diaphragm equations were derived using these assumptions.

The following is a list of variables that will be used throughout this section in defining the various equations:

1. r_d is the diaphragm radius (in.).
2. h is the diaphragm thickness (in.) with the rigid center having a thickness of at least 6h.
3. b is the radius of the rigid center (in.).
4. y is the deflection of the diaphragm center (in.).
5. P is the applied pressure difference (psi).
6. μ is Poisson's ratio for the diaphragm (dimensionless).
7. E is the Modulus of Elasticity for the diaphragm (psi).

8. f_n is the fundamental frequency of the diaphragm (Hz.).

9. W is the specific weight of the diaphragm ($lb/in.^3$).

The characteristic equation for a flat diaphragm with a rigid center is[11]

$$P = \left[\frac{Eh^3y}{Ar_d^4} + \frac{BEhy^3}{r_d^4}\right] \tag{2}$$

where

A = Stiffness coefficient for the linear term

B = Stiffness coefficient for the cubic term

and A and B are found by the following equations[12]:

$$A = \left[\frac{3(1-\mu^2)[1-(b/r_d)^4-4(b/r_d)^2\log(r_d/b)]}{16}\right] \tag{3}$$

$$B = \left[\frac{\left[\frac{(7-\mu)[1+(b/r_d)^4+(b/r_d)^2]}{3}\right] + \left[\frac{(3-\mu)^2(b/r_d)^2}{(1+\mu)}\right]}{(1-\mu)[1-(b/r_d)^4][1-(b/r_d)^2]^2}\right] \tag{4}$$

The frequency characteristics of circular diaphragms are of importance to the transducer designer. In general, a diaphragm's frequency behavior is determined by its many natural frequencies. In terms of a diaphragm's transfer function, these natural frequencies will be located on the imaginary axis. Exciting the diaphragm near these frequencies will set up vibrations which will take a long time to settle out.

Designers pay particular attention to the lowest natural frequency since this frequency determines the useful dynamic range of a transducer. This frequency is denoted f_n and is referred to as the fundamental frequency. The dynamic range of a transducer is then defined in terms of this frequency. One manufacturer states a dynamic range up to 20% of f_n[13]. f_n is found by[14]

$$f_n \approx \left[\frac{9.2200h}{r_d^2}\right]\left[\frac{E}{W(1-\mu^2)}\right]^{1/2} \tag{5}$$

3. Variables and Selections

There are several choices to be made regarding the diaphragm. First, the material chosen will fix the constants E and μ. The thickness h, the radius r_d, and the ratio b/r_d determine the deflection characteristics of the diaphragm. The job of selecting the various dimensions demands detailed knowledge of the requirements.

There is no "best" choice when designing diaphragms. Optimizing the design requires many tradeoffs among the variables. For example, for increased accuracy a designer might consider increasing the radius of the diaphragm, since the deflection distance will increase and make the task of detecting pressures easier. The natural frequency decreases as r_d^2, so increasing the radius may help the accuracy, but at a cost of decreased natural frequency, which limits the useful frequency range of the transducer.

The first thing to choose is the material of the diaphragm. For this study, the design will use Carpenter's Custom 455 Stainless Steel as the diaphragm material. This steel has exceptional high strength and corrosion resistance and is especially designated for diaphragms(15).

Selection of a material for this study is not that critical since the material only gives a baseline for comparison. Carpenter's Custom 455 Stainless is used extensively in commercial transducers so it makes a good choice for this study.

The important physical constants of Carpenter's Custom 455 Stainless Steel are:

1. Modulus of Elasticity, $E = 29.0 \times 10^6$ psi
2. Poisson's ratio, $\mu = 0.31800$
3. Specific Weight, $W = 0.28000$ lb/in.^{3}

The value of 0.10 will be used for the solidity ratio b/r_d. A small b/r_d is desired since larger b/r_d increases the effect of the cubic term in equation 2. For practical purposes, b/r_d only needs to be large enough to reflect all of the light from the transmit fiber.

Inserting the values of E, μ, W, and b/r_d into equations 2, 3, 4, and 5 yields

$$A = 0.16178$$

$$B = 3.44784$$

$$P = 29x10^6 \left[\frac{6.18120h^3y + 3.44784hy^3}{r_d^4}\right] \quad (6)$$

and

$$f_n \approx \left[\frac{98,969.42h}{r_d^2}\right] \quad (7)$$

The objective of diaphragm design is to have as linear a pressure deflection as possible. The criteria to minimize errors requires that the cubic term be limited at the highest pressure. If the cubic term is constrained to be less than 0.05% of the linear term, the maximum deflection allowed, y_{max} is given by

$$y_{max} \leq 0.030h$$

Letting h = 0.030" yields a y_{max} of 0.0009" at 50 psi. Solving for r_d in equation 6 yields

$$r_d = 0.0543"$$

To calculate the diaphragm dimensions that limit the non-linearity to less than 0.025%FS, the following can be used:

1. Select the maximum deflection desired, y_{max}.
2. The thickness of the diaphragm will be given by $h = (y_{max}/0.03)$
3. Select the pressure desired at y_{max}.

4. The radius will be given by

$$r_d = \left[\frac{29.00\text{x}10^6 h^3 y_{max}}{0.16178 P_{max}}\right]^{1/4} \quad (8)$$

Using this method, a number of diaphragms can be easily designed which have the same y_{max}. This will allow one design of the fiber optic detector circuit to be used for a variety of diaphragms.

The dimensions to be used on the 50 psi diaphragm are

$$r_d = 0.543 \text{ in.}$$

$$h = 0.030 \text{ in.}$$

where

$$y_{max} = 0.0009 \text{ in.}$$

The resultant pressure and frequency equations are

$$P = 56{,}919.30y + 35{,}276{,}973.36y^3 \quad (9)$$

$$f_n \approx 10{,}182.04 \text{ Hz.} \quad (10)$$

The best straight line approximation of equation 9 that passes through the origin is

$$P \approx 56{,}940.75y \quad (11)$$

with a maximum error of less than 0.0126%FS. The maximum error occurs at 50 psi and at 25.6 psi.

B Optical Sensor Design

1. Theory of Operation

There are many methods of measuring small distances using optical techniques. For use in pressure transducers, the method chosen needs to be able to measure distances less than a thousandth of an inch. For this study a reflective method is chosen. It is simple, yet highly accurate and reliable.

Figure 5 shows a suggested arrangement for the reflective method. Light is generated and transmitted down a fiber. The fiber is terminated at a distance d from a reflective surface. As the light flux travels down the transmit fiber, the light rays travel at angles ranging from 0° to β (Fig. 6), where β is the largest angle for total internal reflection. As the light goes from the fiber into the air, it disperses at angles ranging from 0 to β_M, where β_M is given by[16]

$$\mathrm{SIN}[\beta_M] = \sqrt{(n_1{}^2-n_2{}^2)}/n_0 \qquad (12)$$

where

n_0 is the index of refraction for the air (1.00)

n_1 is the index of refraction for the fiber core.

n_2 is the index of refraction for the fiber cladding.

Typically, SIN[β_M] is given as the Numerical Aperture of the fiber.

At the reflective surface, the light from the fiber irradiates a circle of light of radius r+a, where r is the radius of the core and a is the additional radius due to the dispersing of the light. It is shown in Fig. 5 that

$$a = d\mathrm{Tan}[\beta_M] \qquad (13)$$

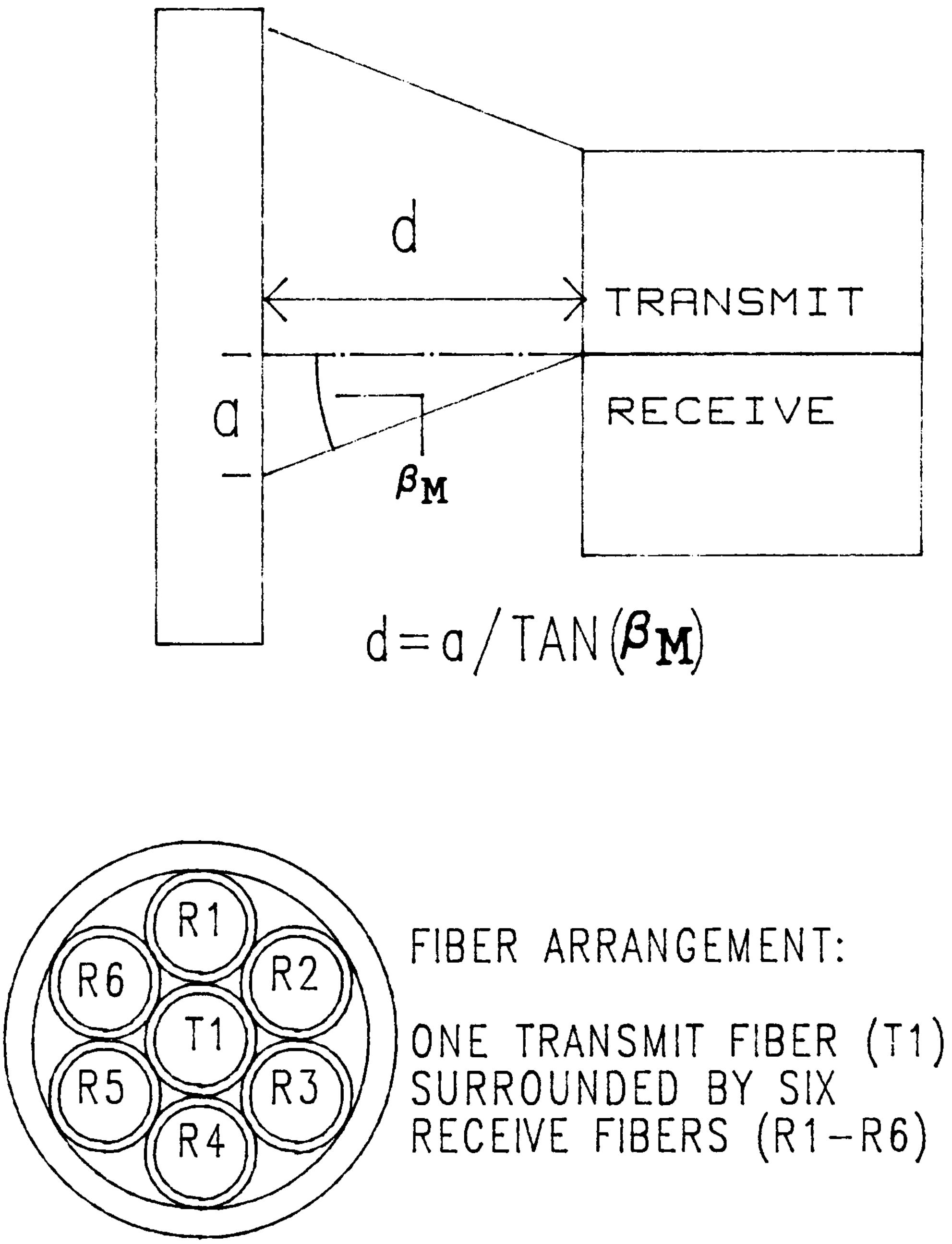

Figure 5: Typical Hardware Arrangement for the Reflective Method of Measuring Distance

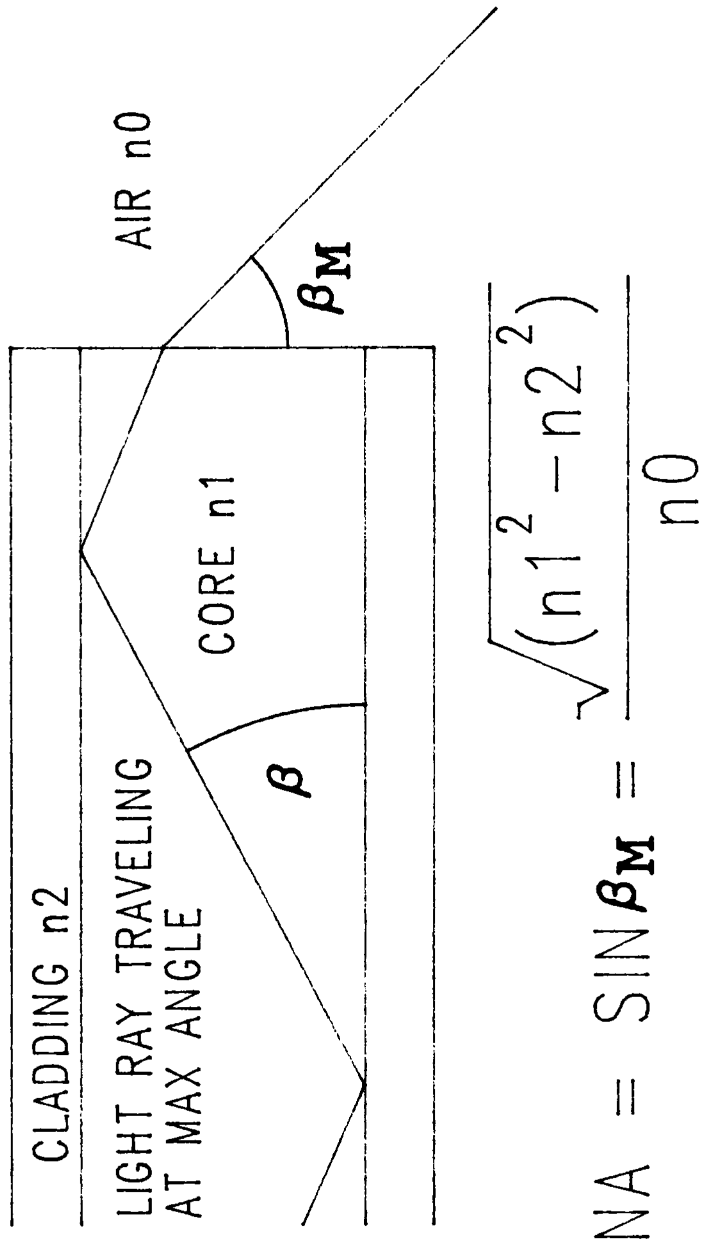

Figure 6: Numerical Aperture Definition

where d is the distance from the fiber to the surface and β_M is the angle of maximum dispersion determined by the Numerical Aperture of the fiber.

The light is reflected off the reflective surface and travels back towards the fibers. The receiving fibers are mounted around the transmit fiber (Fig. 7) in a circular pattern. At the detecting fibers, the flux is distributed in a circle of radius

$$R = r + 2a = r + 2dTAN[\beta_M] \tag{14}$$

Assuming that a negligible amount of flux is lost from the time that the light exits the transmit fiber until the light is seen at the detecting fibers, the amount of flux actually detected by the receiver is proportional to the area of the irradiated light spot that falls on the detecting fibers compared to the total area of the light spot (Fig. 7). The amount of light that the receiving fibers will pick up will depend on the distance d. For d very small, most of the light will be reflected back into the transmit fiber. As d becomes larger, more light is reflected into the receive fibers. At a certain point, the amount of light that the receive fibers pick up will be a maximum. Beyond this d_{max}, the amount of light picked up relative to the total light transmitted will fall off as R becomes greater than the radius of the entire fiber bundle.

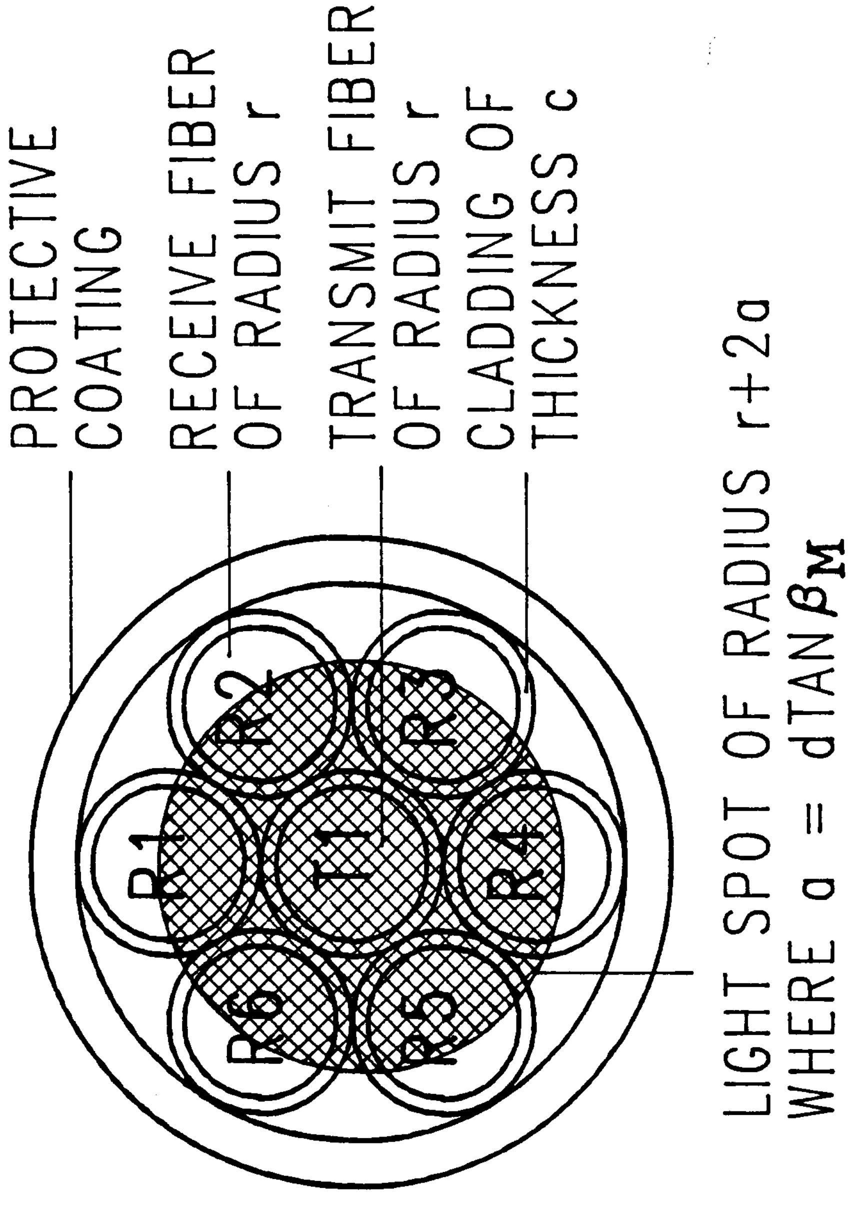

Figure 7: Light Spot as Seen at the Fibers

2. Characteristic Equation

The equation that relates the intensity of the light seen by the receiver has been derived in the appendix. An expression for the intensity of the received light, Φ_R divided by the intensity of the transmitted light, Φ_T was derived and found to be

$$\Omega(z) \equiv \Phi_R/\Phi_T = 0 \qquad \text{for} \quad 0 \le z \le 0.10$$

$$\Omega(z) = 5.3694\left[\frac{\cos^{-1}\left[\dfrac{1.21-(z+z^2)}{1.10}\right] + (1+2z)^2\cos^{-1}\left[\dfrac{1.21-(z+z^2)}{1.10+2.20z}\right]}{\pi(1+2z)^2}\right]$$

$$-5.3694\left[\frac{2\sqrt{1.21-[1.21-(z+z^2)]^2}}{\pi(1+2z)^2}\right]$$

$$\text{for } 0.10 \le z \le 1.10$$

$$\Omega(z) = \left[\frac{5.3694}{(1+2z)^2}\right] \qquad \text{for } z \ge 1.10 \qquad (15)$$

where

$z \equiv a/r$ and

$a = d\mathrm{Tan}[\beta_M]$ = growth in radius of the light spot as it travels a distance d

r = radius of the fiber core (in.)

This equation was derived assuming a cladding thickness of 0.10r.

3. Selections

The light intensity ratio $\Omega(z)$ derived in the appendix has been normalized to r for simplicity. r needs to be selected so that the range of z will be large enough to measure d=0.0009 in. The useful range of z is

$$0.14 \le z \le 0.50$$

This region is selected since the sensitivity to changes in z is maximum (pages 82-86).

The difference in z over the entire useful range is $\delta z=0.36$. Therefore the design requires that a change of 0.36 in z must at least correspond to a change in distance d of 0.0009 in.

This study will use the value of 0.370 for the Numerical Aperture of the fiber. This is a typical value for a silica core fiber.[17] Then

$$\beta_M = \mathrm{SIN}^{-1}[0.370] = 21.716^\circ \tag{16}$$

and

$$\mathrm{TAN}[\beta_M] = 0.3982641 \tag{17}$$

Recalling that

$$a = d\mathrm{TAN}[\beta_M] \tag{13}$$

and substituting the value of $\mathrm{TAN}[\beta_M]$ into equation 13,

$$a = 0.39826d \tag{18}$$

therefore

$$z = a/r = 0.39826d/r \tag{19}$$

with $\delta z=0.36$ and $\delta d=0.0009$ in., r is just

$$r \ge \delta a/\delta z \tag{20}$$

or

$$r \ge (0.0009)(0.39826)/0.36 = 0.0009957 \text{ in.} \tag{21}$$

Let r = 0.0010 in. and the distance d = 0.0009 in. can be measured in the range specified.

With r=0.0010 in. and a=0.39826d, $\Omega(z)$ becomes

$$\Omega(d)=5.3694\left[\frac{\cos^{-1}\left[\frac{1.21-(398.2641d+158{,}614.2972d^2)}{1.10}\right]}{\pi(1+796.5282d)^2}\right]$$

$$+\ 5.3694\left[\frac{\cos^{-1}\left[\frac{1.21+(398.2641d+158{,}614.2972d^2)}{1.10+876.18102d}\right]}{\pi}\right]$$

$$-\ 5.3694\left[\frac{2\sqrt{1.21-[1.21-(398.2641d+158{,}614.2972d^2)]^2}}{\pi(1+796.5282d)^2}\right] \qquad (22)$$

This equation is valid for measuring a δd of 0.0009 in. To find the upper and lower limits in terms of a distance d, recall that

$$z = a/r = d\mathrm{TAN}[\beta_M]/r \qquad (23)$$

or

$$d = rz/\mathrm{TAN}[\beta_M] \qquad (24)$$

With r=0.001" and TAN[β_M]=0.3982641, the values of d for z=0.14 and z=0.50 become

$$d_{low} = 0.000351526 \text{ in.} \qquad (25)$$

$$d_{hi} = 0.001255448 \text{ in.} \qquad (26)$$

and

$$\delta d = d_{hi} - d_{low} = 0.000903923 \text{ in.} \qquad (27)$$

which is large enough for the design requirements.

4. Combined Characteristic Equation

Equations have been derived for the optical sensor and for the pressure sensing diaphragms. The next step is to combine the equations to produce one equation relating the pressure applied and the intensity of the light received by the optical detector.

The equation for the pressure/deflection relationship is

$$P \approx 56{,}940.750y \text{ for the 50psi diaphragm} \tag{11}$$

where y is the deflection distance of the rigid center. This equation for the pressure/deflection is valid with an error of less than 0.0126%FS.

For use as a true absolute transducer, the P=0 point will be at d_{hi}, therefore

$$y=0 \text{ at } d=0.00125$$

and

$$y=0.0009 \text{ at } d=0.00035$$

therefore

$$d = -y + 0.00125 \tag{28}$$

but

$$y \approx P/59{,}940.75 \tag{29}$$

therefore

$$d = -P/59{,}940.75 + 0.00125 \tag{30}$$

Substituting equation 30 into equation 22 yields

$$\Omega_{50}(P)=1.70913\left[\frac{\cos^{-1}\left[\frac{0.46434+0.01326P-4.41467\times10^{-5}P^2}{1.10}\right]}{3.98266-0.05304P+1.76587\times10^{-4}P^2}\right]$$

$$+1.70913\left[\cos^{-1}\left[\frac{1.95565-0.01326P+4.41467\times10^{-5}P^2}{2.19523-0.01462P}\right]\right]$$

$$-1.70913\left[\frac{2\sqrt{1.21-[0.46434+0.01326P-4.41467\times10^{-5}P^2]^2}}{3.98266-0.05304P+1.76587\times10^{-4}P^2}\right] \quad (31)$$

5. Polynomial Expression

While equation 31 is an accurate representation of the pressure/intensity relationship, it is not a useful expression for calculations. Equation 31 will give the intensity for known pressures. What is required is the inverse equation, one which yields the pressure given the intensity.

For practical devices, a polynomial approximation to equation 31 is more easily carried out. Polynomial coefficients can be easily found in the calibration lab by measuring the intensity against standard pressures. The inverse relationship $P=\Omega^{-1}(\Omega)$ of equation 31 could not easily be found analytically.

A sixth order, least squares approximation of equation 31 yields an expression which is accurate to within 0.012%FS[18]. This particular approximation was found using 51 evenly distributed pressures from 0 to 50 psi.

For even greater accuracy, more points could be used. The approximation $P(\Omega)$ is

$$P(\Omega) \approx C_0+C_1\Omega+C_2\Omega^2+C_3\Omega^3+C_4\Omega^4+C_5\Omega^5+C_6\Omega^6 \qquad (32)$$

where

$C_0 = 55.34126499$ $\qquad$ $C_4 = 3240.46660967$

$C_1 = -136.40891001$ $\qquad$ $C_5 = -3802.34114089$

$C_2 = 319.74140394$ $\qquad$ $C_6 = 1279.87592974$

$C_3 = -1476.93363370$

and Ω goes from 0.437122 to 0.042725.

6. Hardware Selection

The hardware necessary to implement the reflective measuring technique consists of a light source, optical fibers, and an optical receiver. These items are readily available on today's market.

The optical cable dimensions have already been discussed. While these dimensions are not a standard cable size, there are manufacturers that specialize in custom built fibers(19).

For the light source, the important characteristic is the amount of optical power available, since the receiver will only see a fraction of the transmitted light. While the amount of light transmitted is important, there are several LED's today that have a high optical power output. For this study, the Hewlett Packard

HFBR 1404 will be discussed, although several other choices exist.

The HFBR 1404 fiber optic transmitter contains an 820 nm GaAlAs emitter[20]. This is an analog device capable of emitting optical power from 0 to over 200 micro-watts (μW). For the optical transducer, the transmitter would be configured to transmit a constant optical signal. The strength of this signal would depend on the receiver characteristics.

The receiver selected for use with the 1404 is the Hewlett Packard HFBR 2404, designed for use with the 1404. The 2404 receiver contains a PIN photodiode and a low noise pre-amplifier integrated circuit[21]. The 2404 receives an optical signal and converts it to an analog voltage. The 2404 is capable of receiving signals from 0 to over 150μW. The responsivity of the 2404 is listed as 7mV/μW. The 2404 has a 0.7 VDC offset associated with it. Since the optical receiver will receive a maximum of 43% of the transmitted signal, the largest received for a 200μW transmit signal would be less than 86μW.

C Filter Design

1. Theory of Operation

As discussed in the diaphragm design section, transducer diaphragms have certain natural frequencies. If properly excited, these poles cause unwanted oscillations of the diaphragms. For this reason, diaphragm designers try to design transducers with the fundamental frequency as high as possible. Transducer manufacturers list the fundamental frequency as a figure of merit, with one manufacturer quoting acceptable response up to 20% of the natural frequency[13].

In practical pressure measuring situations, high frequency pressure waves are not encountered, but very fast transitions between pressures are. If these transitions are fast enough, this can also excite the diaphragm in one of its natural modes. While there is no way to prevent the diaphragm from oscillating, with the proper filtering it is still possible to ascertain the true pressure behavior after the transient has passed. While the diaphragm will oscillate, it will vary about the steady state or low frequency pressures.

A low pass filter would allow the transducer to operate in an environment where fast transitions are expected. The filtering does not raise the dynamic range of frequencies that can be measured. The transducer will still be limited to about 20% of the fundamental frequency in terms of measuring high frequency waves, but the ability to respond to transients will be greatly improved.

2. Filter Selection

Since the objective of this design is to improve accuracy, the filter type selected must be able to maintain the specified gain over the frequency required within a very small margin. An error of less than 0.01%FS is desired for the filter section. The gain must be maintained within this error for frequencies from DC to about 20% f_n. For frequencies above 20% f_n, the gain should decrease monotonically. At f_n, the gain should be negligible. This study will look at a realization using a maximally flat filter which is known ot have these characteristics.

In order to select the filter order, certain criteria must be established. For this design, these criteria are

1. A_{max}, the maximum passband attenuation must be less than 0.01%FS, or 0.000868dB.
2. A_{min}, the minimum stopband attenuation must be greater than 99%FS, or 40dB.
3. The transition region from passband to stopband is defined as from $0.20f_n$ to f_n, or from 2,036Hz to 10,182Hz.

For the maximally flat filter, the filter order needed to satisfy the above criteria is[22]

$$n = \left\lceil \frac{\log[(10^{0.1Amin}-1)/(10^{0.1Amax}-1)]}{2\log(f_n/0.20f_n)} \right\rceil \qquad (33)$$

Substituting the values for A_{max}, A_{min}, and f_n, n becomes 5.5, indicating that a sixth order filter is needed to fulfill the requirements.

The squared magnitude function for the maximally flat approximation is

$$|H(j\phi)|^2 = \left[\frac{1}{1+(\phi)^{2n}}\right] \qquad (34)$$

where ϕ is the frequency w normalized to the 3dB frequency w_c,

$$\phi = w/w_c \qquad (35)$$

With n equal to 6, the ϕ which produces an error of 0.000868dB is found to be 0.492. This requires that the bandpass frequency, $0.20f_n$ be less than 0.492 when transformed to ϕ. The ϕ which produces attenuation greater than 40dB is found to be at 2.15. If $0.20f_n$ is placed at 0.431, then f_n is at 2.15. The actual error at ϕ = 0.431 is 0.0021%FS, which is better than called for.

3. Filter Realization

A sixth order maximally flat filter has been selected to meet the design requirements. The normalized transfer function can be written, using Butterworth polynomials, as[23]

$$H(s^*)=\left[\frac{K}{(1+0.518s^*+s^{*2})(1+1.414s^*+s^{*2})(1+1.932s^*+s^{*2})}\right] \qquad (36)$$

where s^* is the normalized s, or

$$s^* = s/w_c \tag{37}$$

In this design,

$$w_c \approx 29{,}687$$

H(s) can be realized using active RC filters. The most common approach is to use three cascaded second order filters[24]. The second order circuit is shown in Fig. 8. The values of the components determine the pole locations of H(s). Consider the sixth order function H(s) to be the product of three second order functions, or

$$H(s) = H_1(s)H_2(s)H_3(s) \tag{38}$$

where each $H_i(s)$ has the following transfer function:

$$H_i(s) = \left[\frac{K_i a_0}{s^2+a_1 s+a_0}\right] \tag{39}$$

The overall gain of the filter is just

$$K = K_1K_2K_3 \tag{40}$$

where the K_i's are determined by the individual stages of the filter. The K_i's must be limited for stable operation[25].

The input signal from the optical receiver is an analog voltage from 0.7V to 1.2V. If the voltage offset (0.7V) is subtracted, the input signal V_i satisfies

$$0.0V \leq V_i \leq 0.5V$$

It is desirable to have the output signal, V_o, between zero and fifteen volts. This maximizes the resolution of the signal before an A/D conversion is done.

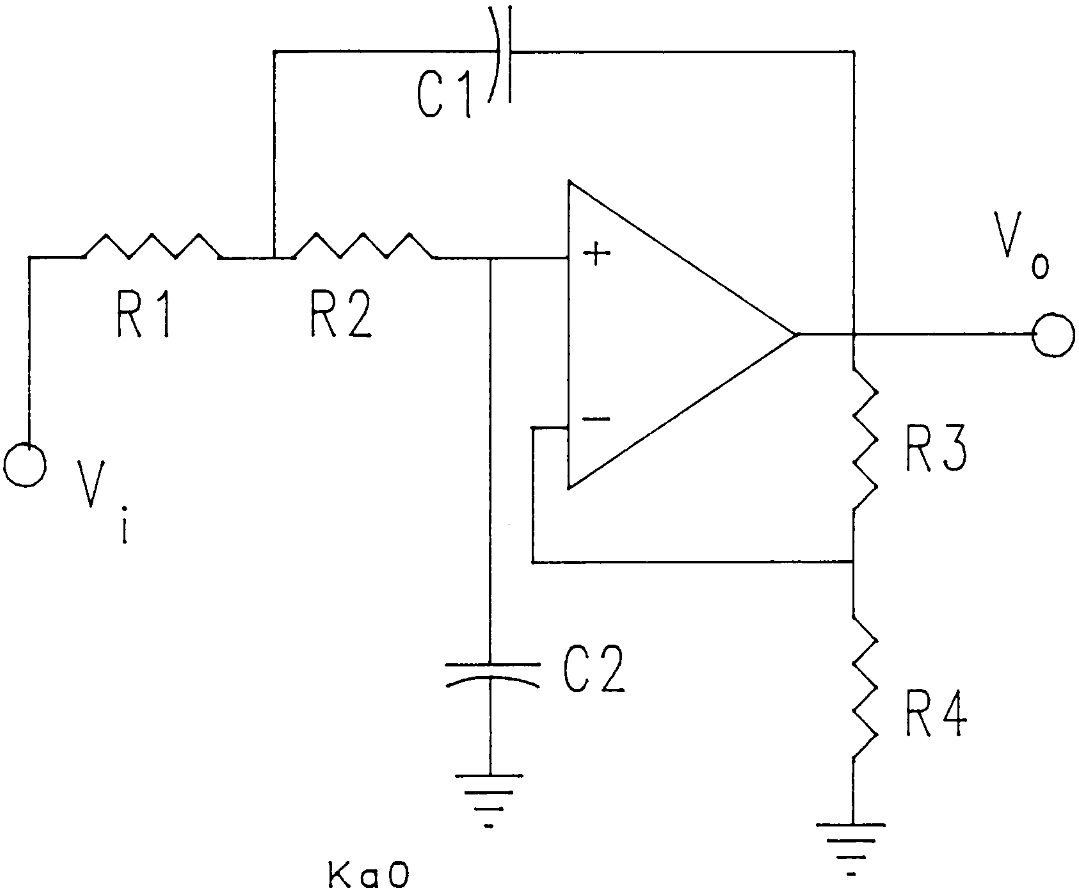

$$H(s) = \frac{Ka0}{s^2 + a1s + a0}$$

$$a0 = \frac{1}{R1R2C1C2}$$

$$a1 = \frac{1}{R1C1} + \frac{1}{R2C1} + \frac{(1-K)}{R2C2}$$

$$K = (1 + R3/R4)$$

Figure 8: A Second Order Active Filter

The gain K that is necessary for this conversion is just

$$K = 10.0V/0.5V = 20.00$$

By using standard resistor values, a gain of 19.60 is possible with

$$K_1 = K_2 = 2.80$$

$$K_3 = 2.50$$

Referring to the second order circuit (Fig.8), $H_i(s)$ is

$$H_i(s) = \left[\frac{K_i a_0}{s^2+a_1 s+a_0}\right] \tag{41}$$

or

$$H_i(s) = \left[\frac{K_i G_1 S_1 G_2 S_2}{s^2+s(G_1S_1+G_2S_1+G_2S_2-KG_2S_2)+G_1S_1G_2S_2}\right] \tag{42}$$

where $G_1=1/R_1$, $S_1=1/C_1$, $G_2=1/R_2$, and $S_2=1/C_2$.

Matching coefficients,

$$a_0 = 1/R_1R_2C_1C_2 \tag{43}$$

$$a_1 = 1/R_1C_1 + 1/R_2C_1 + 1/R_2C_2(1-K) \tag{44}$$

Since there are only two values to specify the filter but four components, there are two degrees of freedom in the selection of components. Typically, the capacitors are chosen to be of equal value to minimize the capacitance spread[26]; the capacitor size would then be chosen for convenience.

A solution of the 6th order filter is shown in Figure 9. There is no unique solution for the filter and

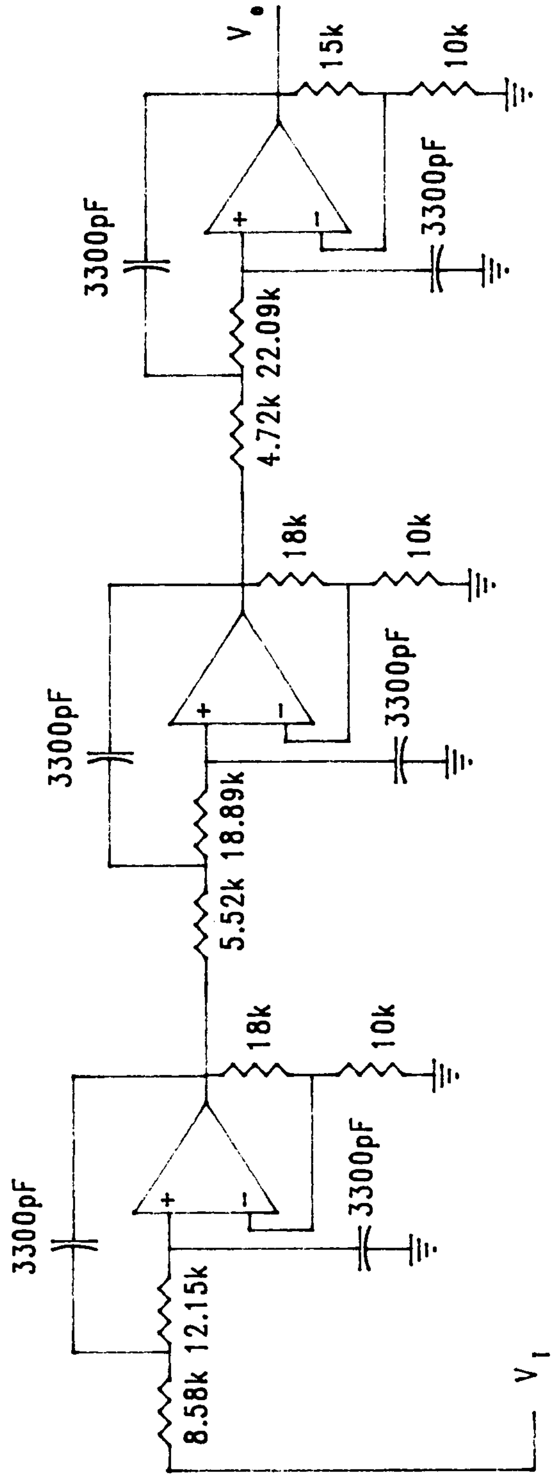

$$H(s) = \frac{19.6}{(s^2 + 0.5176s + 1)(s^2 + 1.4142s + 1)(s^2 + 1.9318s + 1)}$$

$H(s)$ normalized to the cutoff frequency w_c, where

$$w_c = 29{,}687$$

Figure 9: A Sixth Order Butterworth Filter

the filter lends itself very nicely to integrated circuit realization in a large scale production situation.

In terms of discrete components, the selection of the Op Amps is critical. To be consistent with the transducer design, the Op Amps must be high accuracy, low noise devices. The AD OP-27 Op Amp by Analog Devices has a worst case noise of 80 nV p-p and a drift of less than 0.2 μV/month[27].

D Microprocessor Circuit

1. Theory of Operation

The theory of operation for the microprocessor circuit is relatively simple. The output signal from the filter circuit is a voltage, V_o between zero and fifteen. The equation that relates the applied pressure to V_o is

$$P(V_o) = C_0+C_1V_o+C_2V_o^2+C_3V_o^3+C_4V_o^4+C_5V_o^5+C_6V_o^6 \qquad (45)$$

where

$C_0 = 5.53413\times10^1$ $\qquad C_4 = 5.71572\times10^{-3}$

$C_1 = -4.97117\times10^0$ $\qquad C_5 = -2.44416\times10^{-4}$

$C_2 = 4.24649\times10^{-1}$ $\qquad C_6 = 2.99822\times10^{-6}$

$C_3 = -7.14840\times10^{-2}$

Fig. 10 shows the pressure/voltage relationship. This signal is sent through an A/D Converter which converts the analog voltage to digital representation in binary form. The output of the A/D is fed to a microprocessor which

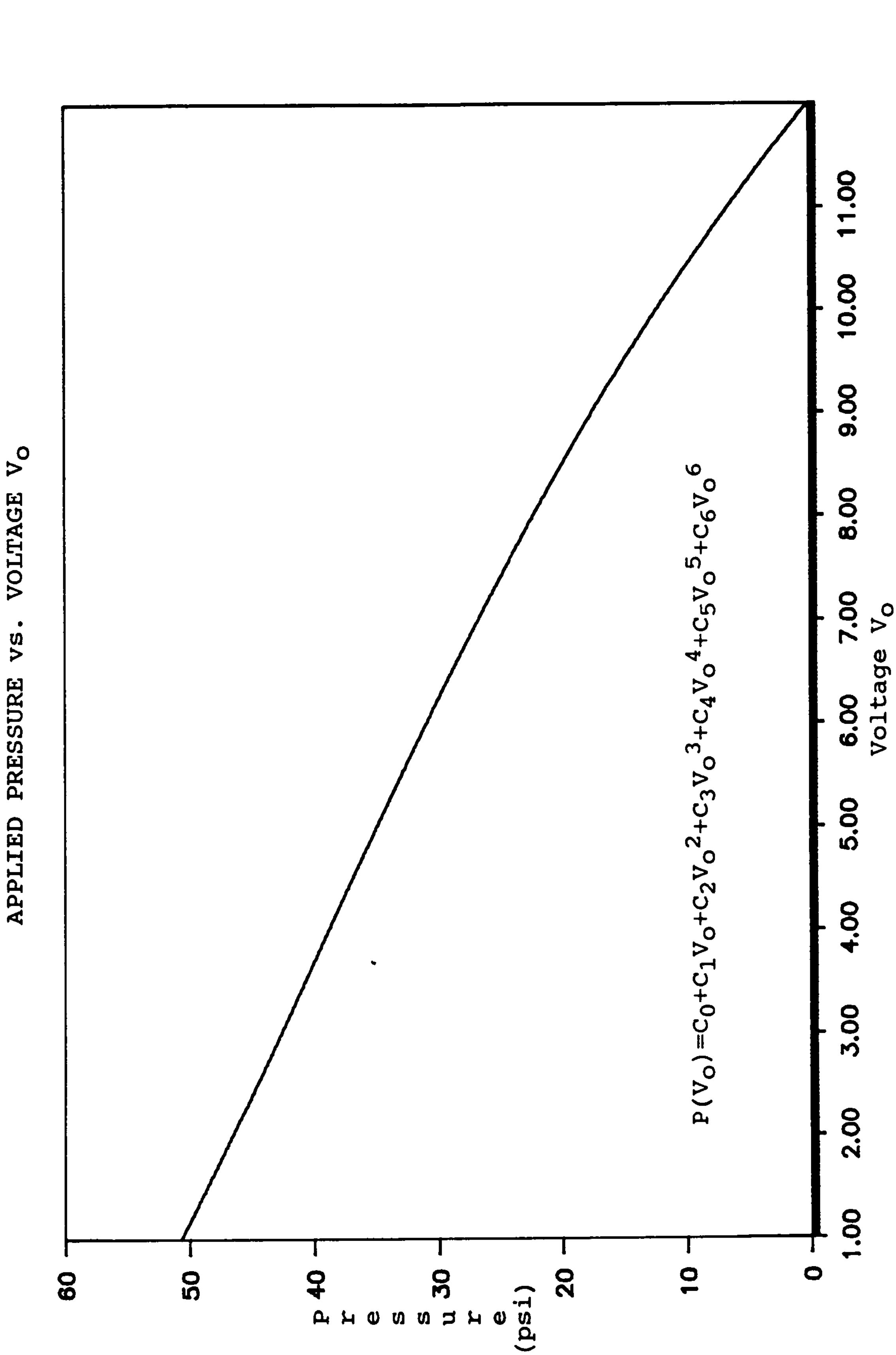

Figure 10: The Pressure/Voltage Relationship

converts the digital signal to a digital output that represents the pressure applied to the device.

The microprocessor could be used for many other functions as well as for conversion of the deflection data into pressure data. For example, the microprocessor might be used as a controller for the entire pressure device. The intensity of the optical input signal could be varied via the microprocessor. The gain on the amplifiers could be actively controlled. The microprocessor could also be used as a digital filter for the deflection data, given that enough information is known about the deflection characteristics.

2. Circuit Design

The microprocessor circuit can be broken down into two parts, A/D conversion and microprocessor data conversion. Each area will be considered separately.

There are many A/D converters on the market today that can do the task. The choice becomes one between accuracy and conversion time. Basically, A/D converters can be considered to be as accurate as one half the value of the least significant bit (LSB)[28].

Since the accuracy of the optical pressure transducer is of primary importance, the designer must establish the maximum allowable error that the A/D converter can contribute to the system. This error will decide how many bits of conversion are needed.

For the fiber optic transducer, a 12 bit A/D converter is accurate to within ±0.0122%FS. This should be accurate enough for many applications. A 14 bit A/D converter yields accuracies of ±0.00305%FS. Since the objective of this design is to minimize error, the 14 bit A/D converter will be used. Along with the accuracy of the A/D converter, concern must be given the conversion time. Conversion times run from as low as 1 μsecond up to 100 μseconds. In general, the time for conversion increases with the demand for more bits. Analog Devices has a converter (AD ADC71) which does a 14 bit conversion in 45 μseconds and has a microprocessor interface built in[29]. If a 12 bit converter is used at the expense of higher error, the conversion time drops to 5 μseconds (AD5240)[30]. For this study, the AD ADC71 converter will be used.

There are so many microprocessors on the market today that the field is not narrowed down by the given design requirements. For purposes of this study, the important considerations are:

1. Math processing capability. The microprocessor's primary function is to convert the input into a linear representation of the applied pressure.

2. Input/Output capabilities. Due to the number of bits required for I/O.
3. Clock speed. How fast can it do a conversion and output it.
4. Control capabilities.

First, the choice of machine size must be made. An 8 bit machine could be used, but the input signal (14 bits from the A/D) would have to be sent as two bytes, thus requiring two ports or sharing one port and multiplexing the data into the microprocessor. If the machine is fast enough and powerful enough, then an 8 bit machine would be acceptable. A 16 bit machine would have large enough I/O ports to avoid any multiplexing or multi-porting schemes. For the purposes of the this study, a 16 bit machine is the logical choice.

The math processing capability of the microprocessor is of primary importance. The conversion of $P(V_O)$ to a linear pressure representation is not trivial. The equation for $P(V_O)$ is a sixth order polynomial, so the coefficients must be stored in the microprocessor. As well as being stored, they must be periodically changed during calibration, indicating the need for some RAM on the microprocessor.

One possible solution for the optical transducer is the Intel 8086 Microprocessor with an 8087 Numeric Data Coprocessor[31]. The coprocessor is necessary for the sixth order polynomial curve fit. The 8087 supports 32, 64, and 80 bit floating point arithmetic, so the precision of the curve fit will be very good. In order to obtain this precision, time is sacrificed since floating point arithmetic is slow. The total time to do the digital conversion will be over 100 μseconds. The design of the transducer is not driven by any high speed requirements, so the choice of the 8086/8087 system is a good one.

Another possible solution for the optical transducer is the TMS32010 Digital Signal Processor by Texas Instruments[32]. The feature that makes the TMS32010 attractive for this application is it's speed. The TMS32010 can perform a double-precision multiplication in 200 nsec. Unfortunately, the TMS32010 only supports fixed point arithmetic, and the precision lost on a sixth order curve fit is too great for the transducer design.

3. Software Requirements

The processor for the optical transducer must be able to perform several functions. First, it must be able to do the conversion of the digital signal to a digital pressure representation. This consists of forming a sixth order polynomial from the input signal.

The processor must be able to calculate the polynomial coefficients during calibrations. This consists of a routine that can do a least squares approximation[18] of the input from the filter circuit for a given set of known input pressures. The coefficients of this calculation are known as the calibration coefficients. There is no set time requirement for this routine since calibrations are typically done at a laboratory under very stable conditions.

A third routine that is important is a re-zero routine which calculates and stores the constant coefficient of the sixth order curve fit. During operational use of the optical transducer, a random drift of the transducer's electronics will cause accuracy problems if there is no way to compensate. The drift can become significant. A periodic re-zero consists of applying a vacuum to the transducer and computing the constant term of the sixth order equation. Since drift affects the entire equation, correcting the constant term corrects the entire equation. In a practical situation, the transducer might be re-zeroed every two hours to maintain system accuracy.

Another routine might send out all of the calibration coefficients through the output port. Still other routines are possible depending on application and sophistication of the device.

The algorithms for the conversion routine, the calibration routine, and the re-zero routine are shown in Figures 11, 12, and 13.

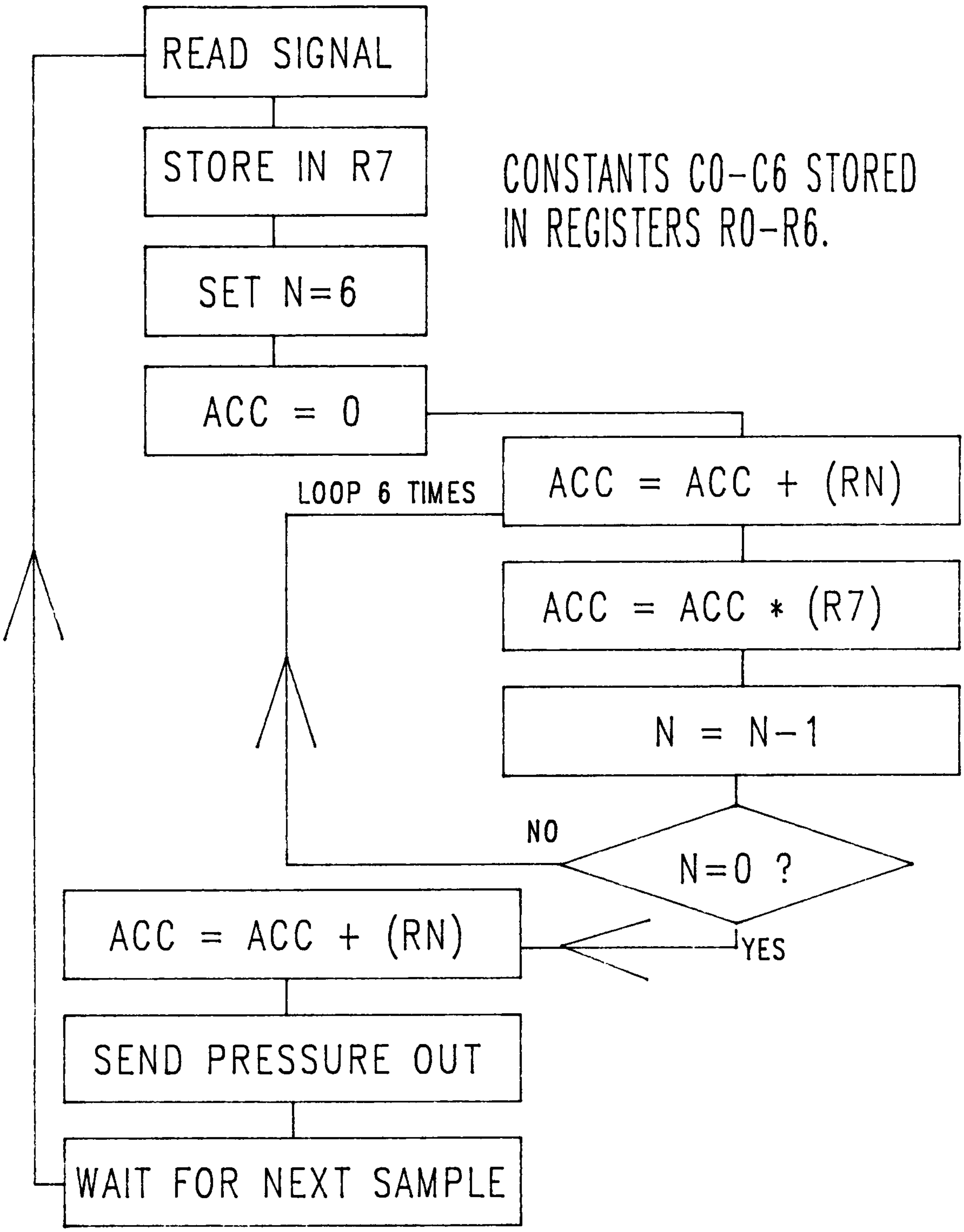

Figure 11: Software Algorithm for the

Data Acquisition

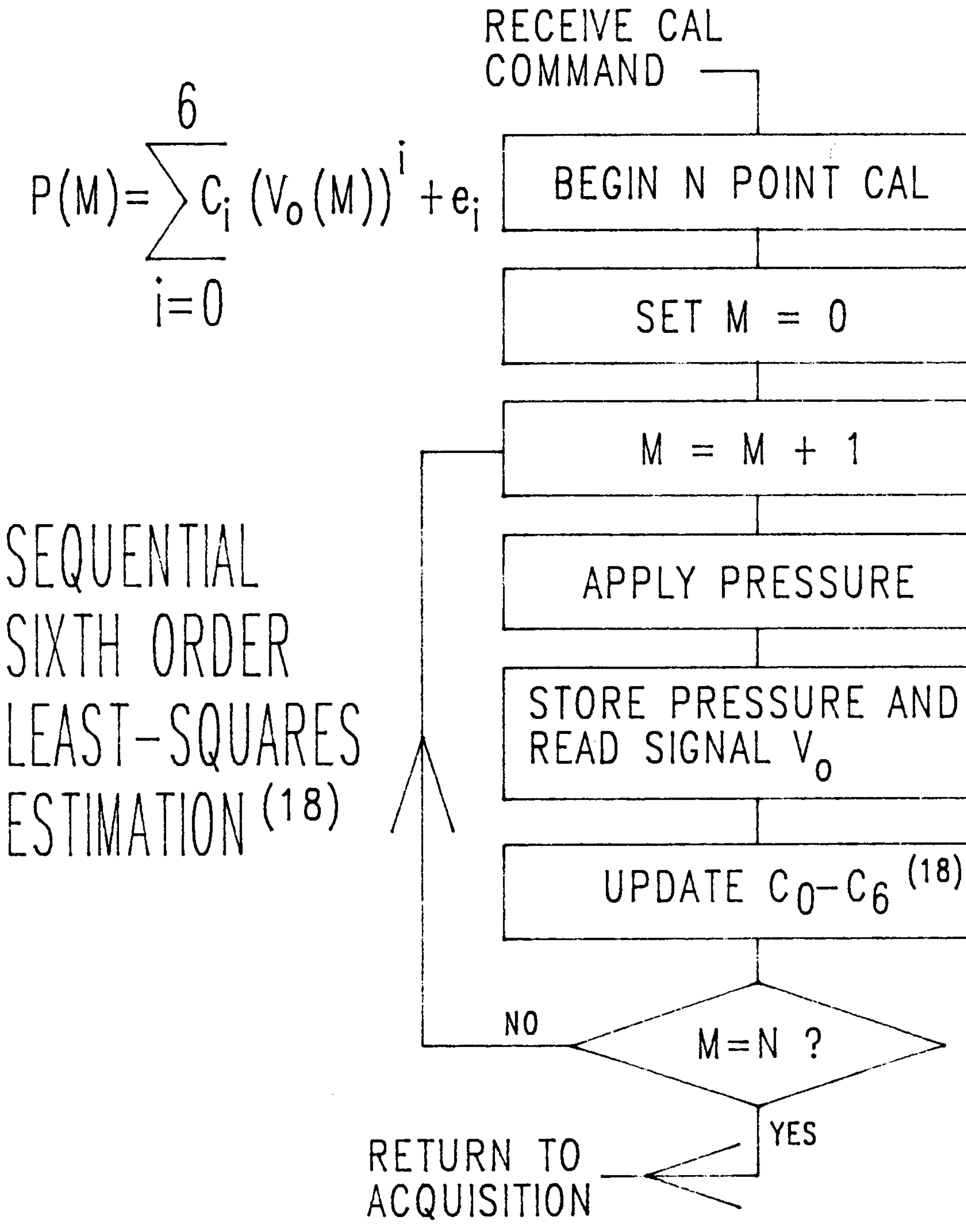

Figure 12: Software Algorithm for the

Calibration Routine

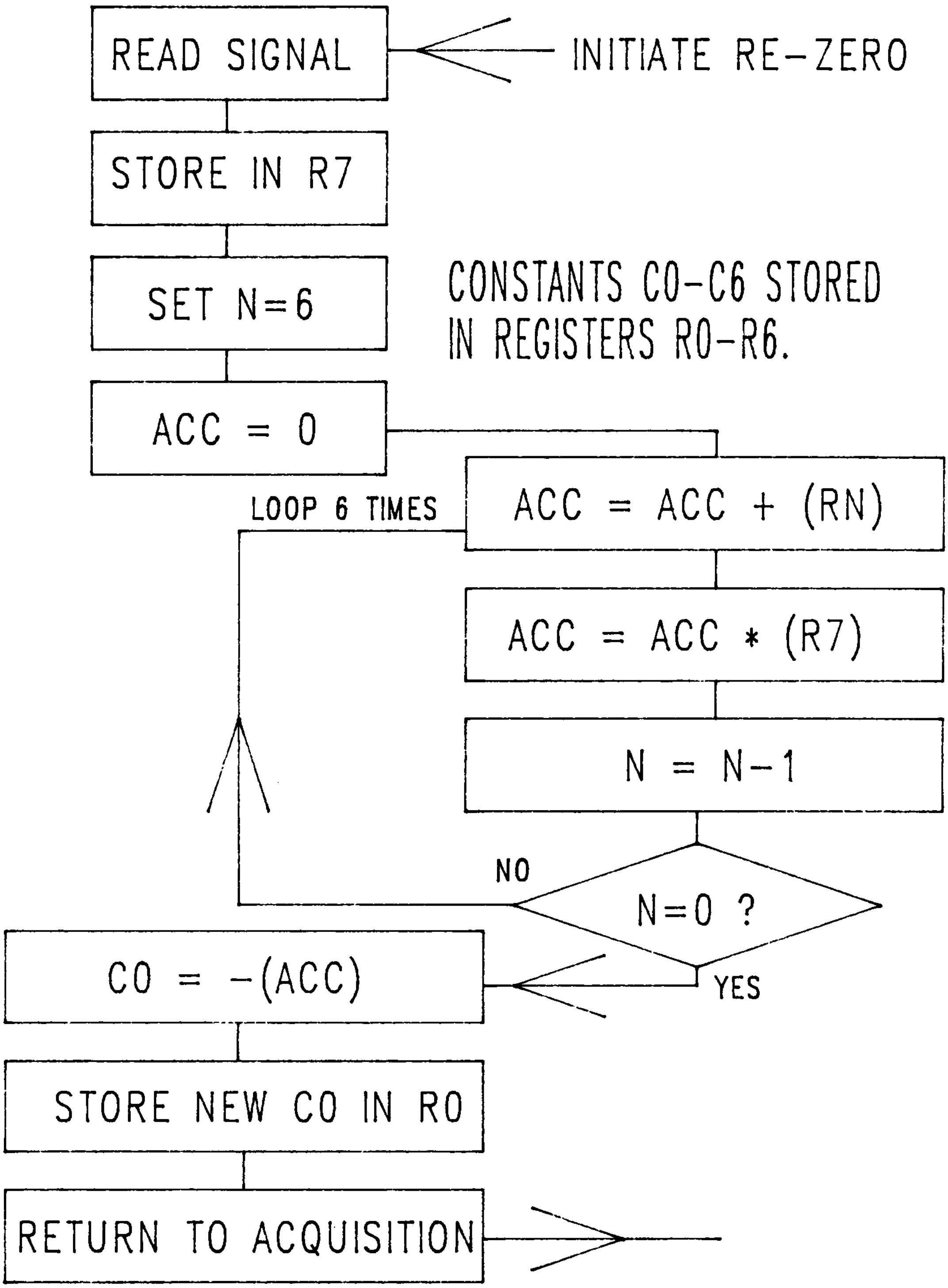

Figure 13: Software Algorithm for the Re-Zero Routine

E Temperature Protection

1. Theory of Operation

In many transducers, there is a considerable change in characteristics as the temperature changes. The resistivity of components changes, voltage levels experience shifts, the diaphragm contracts and expands with temperature. The end result is an overall shift in transducer performance as the temperature changes. Usually, the amount of change in performance is listed as a percentage of full scale per degree Fahrenheit (%FS/°F).

Many transducers use additional circuitry in an attempt to offset some of the temperature effects. With standard transducers, it is not possible to protect the circuitry from the thermal changes. The circuitry of standard transducers such as a strain gauge is physically attached to the diaphragm, so the circuitry will essentially see the environment that the diaphragm does.

One great advantage of the optical transducer is the complete isolation of the electronics from the diaphragm. This means that the electronics can be isolated from any adverse thermal conditions. In this manner, only the diaphragm is affected by thermal effects. This greatly reduces the thermal sensitivity of the transducer.

2. Method of Protection

There are different ways to isolate the electronics from the thermal conditions surrounding the transducer. The easiest method is to simply move the electronic circuitry to a remote, temperature controlled environment. The only requirement is for the fiber optic cables to carry the light to and from the diaphragm. In many situations, this would be a desirable setup, since control of the transducer would be in a controlled environment while the actual pressures being measured might be in an inaccessible and harsh environment, such as in a turbine engine test cell.

Another method of isolating the electronics from the environment is to enclose the electronics in an aluminum case with an internal heating element that would maintain the temperature of the case at some specified temperature. This method is often used when the entire device must exist in the environment.

Still another method is to surround the electronics with some sort of liquid cooling jacket. While this method is occasionally used, it is more sensitive to temperature. Water must also be supplied, adding extra requirements to the transducer design.

While the thermal protection is simple, it is important for the transducer's proper operation.

3. Thermal Characteristics

All of the components listed for use in the design of the optical transducer have thermal characteristics. Of primary significance is the diaphragm's thermal sensitivity. The sensitivity of the diaphragm to temperature is a function of the material chosen. The sensitivity of the diaphragm can be written as[33]

$$s_T = [1-(1+\alpha)/(1+c_e)] \tag{46}$$

where s_T is the thermal sensitivity in %FS/°F, α is the average thermal coefficient of expansion, and c_e is the average thermal Modulus of Elasticity. For Carpenters Custom 455 Stainless, α is $6.20\text{x}10^{-6}$ in./in./°F and c_e is $-15.5\text{x}10^{-5}$ psi/psi/°F[34]. Substituting these values into the equation for s_T yields

$$s_T = -0.00032\%\text{FS}/°\text{F}$$

This is a relatively small error compared to many other standard transducers. For even better temperature sensitivity, consider the alloy Ni-SPAN-C 902. It has a constant Modulus of Elasticity from -50°F to +150°F, or c_e is zero in that range. For diaphragms built with this alloy, s_T becomes

$$s_T = -9.00\text{x}10^{-6}\%\text{FS}/°\text{F}$$

This means that a one hundred degree shift would introduce an error of less than -0.0009%FS!

CHAPTER III

TRANSDUCER CHARACTERISTICS

A Error Analysis

The main purpose of this study is to show that a pressure transducer design using the optical reflective technique will yield higher accuracies than transducers that use standard techniques. An analysis of the Optical Pressure Transducer will reveal where the uncertainties in the system lie and what the limits on these uncertainties are. Throughout this section, all errors will be converted to %FS. This allows the component errors to be combined to yield the total system error.

1. Diaphragm Error

The diaphragm was shown to have a cubic deflection/pressure relationship. The system design assumes that this relationship is linear, thereby introducing an error into the system. This error is known as the non-linearity of the diaphragm. Using a straight line approximation, the maximum error is one half the magnitude of the cubic term at y_{max}. For the optical transducer, these errors are less than .0126%FS (page 16).

Another area of concern for the diaphragm is its dimensions. The specification for a 50 psi diaphragm calls for a radius of 0.540 in. and a thickness of 0.030

in. The approximation for this diaphragm is

$$P \approx 56{,}940.750y \tag{11}$$

where y varies from 0.00 in. to 0.00090 in. This equation yields an error no greater than 0.0126%FS, or 0.0063 psi. This approximation assumes the diaphragm dimensions are accurate, but in a practical sense the ability to machine a diaphragm to within 0.0001 in. is nearly impossible, or at least very expensive.

The fact that the diaphragm dimensions may be off by a thousandth of an inch does not degrade the accuracy of the diaphragm. It just means that the approximation necessary to maintain a maximum error of 0.0126%FS must be found. In practical transducers, this is accomplished by calibrating the transducer at the manufacturer, obtaining the best straight line approximation of the diaphragm and shipping the transducer along with its characteristic equation and calibration coefficients. It is valid to assume the approximation is valid, but in industry, this approximation is found in the laboratory, not theoretically.

Hysteresis is another contributor to error in a diaphragm. Hysteresis occurs when the deflection distance takes on two distinct values for the same applied pressure. The deflection depends on whether the pressure is being applied in an increasing or decreasing manner[35].

Hysteresis is a property of metallic compounds due to their molecular structure. It is not possible to calculate hysteresis theoretically, but certain stainless steels exhibit lower hysteresis effects than others. The forming and annealing processes used also determine the hysteresis characteristics.

Although the hysteresis can't be calculated, the amount of hysteresis depends on the deflection distance of the diaphragm and is generally much smaller than the non-linearity of the diaphragm. Since the non-linearity error already specifies a band of error less than 0.0126%FS, as long as the hysteresis falls within that band, it adds very little to the error.

In practical transducers, hysteresis is measured by applying pressures in an increasing, then decreasing manner and recording the outputs. The best straight line approximation includes the effects of hysteresis.

In cases where hysteresis cannot be tolerated, measurements will be made only after the transducer has been pulled to reference. In this manner, the diaphragm sees all measurements as an increase in pressure and occur only on one side of the hysteresis curve.

The last contributor to diaphragm error is that of repeatability. The repeatability of a transducer is a measure of how accurately a transducer repeats the same output for the same applied input. In common transducers today, the repeatability errors are caused by the physical devices that are attached to the diaphragm. In strain gage transducers, the strain gage is bonded across the diaphragm as well as to the transducer wall. This bonding affects the diaphragms characteristic equation and acts as a damper. The ability of the diaphragm to repeat accurately is hampered by attaching devices to it. One great advantage in the Optical Pressure Transducer design is that there is no physical connection between the diaphragm and the rest of the transducer. The diaphragm's repeatability characteristics only depend on the dimensions and the material of the diaphragm. Repeatability of the diaphragm should be excellent, well within the 0.0126%FS specified for the non-linearity.

The combined total error of the diaphragm should be less than 0.020%FS. This allows for some additional error due to the effects of hysteresis and repeatability as well as the non-linearity.

2. Optical Sensor Error

The optical sensor equation which relates the intensity of the received light to the distance measured was derived in the appendix. The losses expected in such a system are discussed in the appendix as well. While these losses are significant and even unpredictable, they affect only the gain of the system, not the terms of the equation. Any lost gain can easily be recaptured in the filter circuit.

Although these losses are unknown, they will remain constant, or at least change very slowly with time, over months. Periodic calibrations will easily compensate for these changes and reduce their effects on the transducer to insignificant proportions.

Other losses must be considered that may affect the terms of the characteristic equation derived in the appendix. Such losses concern the light producing and receiving devices used.

The light source can be considered a current device which converts most of the received current to light. For the optical transducer design, a constant source of light is desired. Any fluctuations in the intensity of the light source yields errors in the received light function. Light sources are rated for their ability to convert current to light by an efficiency rating, the percentage of current converted to light. Fluctuations in this efficiency are intolerable. With today's hardware, the requirement for a constant light source is easily met.

Similarly, the receiver converts light to a current at a certain efficiency and fluctuations would also introduce errors.

Fluctuations occur in the light source and receiver due to several factors. Either the efficiency of the source, or the amount of current can change. First, the light sources and receivers on the market today are temperature sensitive. The efficiency of the device will change as temperature changes. This change is not linear and not easily compensated for. The amount of current supplied to the source could change due to temperature swings as well. Typically, the light source and the receiver are a matched pair, often fabricated on the same silicon chip to match their characteristics as closely as possible.

In order to assure a constant light source and current source, a heater could be used to raise the electronic components to a known temperature (page 45). This would ensure constant performance over a certain temperature range, thereby eliminating thermal drift.

A significant loss due to the optical circuit is the output noise from the receiver. The output noise level is listed as 0.25 mvolts. With a maximum ouput of 1.3 volts, this is an error of 0.019%FS.

With the exception of noise errors, the errors due to the optical sensor should be negligible. This is the main advantage of this design. Optical circuits are extremely accurate, reliable, and repeatable. They make an excellent choice in all types of instrumentation including pressure transducers.

3. Filter Circuit

The error due to the filter is determined by the falloff in gain as higher frequencies are being measured. The worst case occurs at $0.20f_n$, which is the largest frequency that the transducer was designed to measure dynamically. The loss at this frequency was shown to be less than 0.0021%FS. For static measurements, there is no loss of gain, hence no error.

Another source of error in the filter circuit is the noise. The Op Amps selected were chosen for their extremely low noise characteristic. The AD OP-27 has less than 80 nV of noise, worst case. If you consider the input signal to the first stage of the filter to be the worst case, the error introduced by the noise is less than 0.00013%FS, with a 0.5 V signal being considered as Full Scale. This indicates that the effects of noise in the filter circuit are almost negligible.

4. Microprocessor Circuit

In the microprocessor circuit, the errors can be attributed to the A/D converter, the microprocessor, and to the noise and drift within the circuit.

As shown in the design section, the error introduced by the A/D converter is equal to one half the magnitude of the least significant bit. For a 14 bit converter, this was found to be less than 0.003%FS. If less accuracy can be tolerated, the conversion can be done using a 12 bit or less converter. The trade off becomes one of conversion time versus accuracy. Since accuracy is the main objective, the 14 bit converter was selected.

The errors attributed to the microprocessor have to do with the numerical limitations of a digital system. First, the sixth order curve fit will introduce an error of 0.012%FS (page 26).

Since the processor has to perform a sixth order curve fit, and the processor is limited by word size, there is an error introduced as significant bits are lost due to the various multiplications and additions in the curve fit routine. One way to minimize the error is to use a math coprocessor that can do floating point arithmetic. This method is slower than using fixed point arithmetic, but the ability to maintain the maximum number of bits of significance is more important than speed.

Using the floating point format, it is possible to carry 24 bits of precision throughout the calculations. This indicates that the error due to the processor is insignificant.

There will also be an error created when the pressure is output. If the pressure is converted to a 16 bit number to accommodate the processor port size, the error induced will be 0.000031%FS. Again, this is almost negligible compared to the other errors.

5. Transducer Drift

Drift is a characteristic that cannot be compensated for. Drift will occur slowly over time. As stated before, the effects of drift can be overcome by changing the coefficients of the curve fit routine in the processor. Since drift occurs over time, usually over a period of hours, periodic re-zeroing of the transducer will assure that system accuracy is being maintained.

6. Total System Error

The total system error is just the square root of the sum of the square of the component errors. The component errors are as follows:

1. Diaphragm error ≤ 0.020%FS
2. Optical Sensor error ≤ 0.019%FS
3. Filter gain error ≤ 0.0021%FS
4. Filter noise error ≤ 0.00013%FS
5. Curve fit error ≤ 0.012%FS
6. A/D Converter error ≤ 0.003%FS
7. Output error ≤ 0.000031%FS

TOTAL ERROR ≤ 0.03031%FS

This shows that the total error expected in such a design could be less than 0.031%FS.

The reflective transducer would actually have much better error terms in a practical situation. This study assumed that errors were introduced by the assumption about diaphragm linearity and by the conversion from the actual intensity transfer function to the sixth order curve. The study counted each of those errors separately and added them into the total error, but in a real transducer, the calibration coefficients would be measured against the actual pressure/intensity relationship, not against theoretical curves. The actual curve fit will decrease the total system error.

B Summary of Transducer Characteristics

1. Transducer Error

As discussed in the previous section, the error for the optical transducer will be less than 0.024%FS, which is less than 0.012 psi on a 50 psi transducer.

2. Frequency Characteristics

This transducer has been designed to measure dynamic pressures up to about 2,036 Hz. Due to limitations in the diaphragm, this transducer shouldn't be operated above this frequency. Special circuitry has been added to allow for the measurements of fast transients (fluctuations in pressure that occur in less than 500 μseconds).

The natural frequency for this transducer was found to be approximately 10,182 Hz.

3. Thermal Drift

Due to the electrical isolation of the diaphragm from the rest of the transducer, the thermal drift can be stated to be less than -0.00032%FS/°F, or -0.00016psi/°F.

If a different diaphragm material is considered, such as Ni-SPAN-C 902, the thermal drift is less than -9.00×10^{-6}%FS/°F, or 4.5×10^{-6}psi/°F.

4. Transducer Range

This particular design is for a 0 to 50 psia transducer, although the design technique will allow for design of a wide variety of ranges.

5. Sample Rate

The speed at which the transducer can sample the pressures is limited by the microprocessor. While the A/D converter can do a conversion in 45 μseconds, the processor will take over 100 μseconds to do the sixth order curve fit. The actual time is probably close to 150 μseconds to do the conversion. The total conversion time of one pressure would be about 200 μseconds. The times for all of the other circuitry is insignificant compared to the processor time. With a 200 μsecond conversion time, the sample rate will be about 5,000 samples/second.

CHAPTER IV

CONCLUSIONS

A Comparisons

Before direct comparisons can be made between current commercial transducers and the optical transducer, some explanation is necessary. There are many different types of commercial transducers available today. They are categorized by accuracy, type of conversion used, cost, and other distinguishing characteristics. In general, the cost and the accuracy of a transducer are very closely related. The intent of this study is to show that not only is the optical transducer feasible, it is also attractive from a cost standpoint. The cost to build a prototype reflective transducer would be about $600. This includes the retail costs of all of the components. In a manufacturing environment, the component costs would decrease but other manufacturing costs would be incurred. Table 1 contains some direct comparisons between some commercial transducers and the optical transducer. Costs have been included where known to give the reader a feel for the expense involved in making accurate pressure measurements.

The optical transducer offers better characteristics in virtually every important category. The error is

Table 1: Comparisons between the Optical Transducer and Commercial Transducers

Model vs. Specs.	Optical Design	Setra 204 (35)	Setra 250 (35)	Setra 270 (35)	MKS 390 (36)	Gould PL822 (13)	Shaevitz P-3061 (37)	Shaevitz P-700 (38)
Transducer Type	Optical	Capac.	Capac.	Capac.	Capac.	Strain Gage	Induct.	Strain Gage
Range	0-50psi	0-50psi	0-30psi	0-50psi	0-20psi	0-50psi	0-50psi	0-50psi
Error %FS	0.030	0.11	0.07	0.07	0.08	0.40	0.50	0.30
Thermal Shift %FS/°F	0.00032	0.003	0.001	0.001	0.002	0.005	0.020	0.008
Thermal Zero Shift	0.0	0.004	0.001	0.001	0.0007	0.005	0.020	0.008
Natural Frequency kHz	10	2.5	N/A	N/A	unk	5	N/A	5
Response Time mseconds	0.5	1	20	10	40	unk	unk	unk
Diaphragm Material	Carpen. 455 SS	SS	Quartz	Ceramic	Inconel 304SS	17-4PH SS	NI-SPAN-C 902	17-4PH SS
Cost($)	≈600	695	1,265	1,050	1,500	unk	558	681

decreased by over a factor of two over most of the transducers listed. Even the MKS 390 cannot meet the optical transducer's error specification although the MKS 390 is considered to be a high accuracy instrument.

The natural frequency of the optical transducer is increased by a factor of two over the standard transducers as well. This means an increased dynamic range of the device. The filtering also provides additional capability that none of the others offer.

The thermal shift of the optical transducer is decreased by a factor of over three. This could be improved by using another diaphragm material, such as Ni-SPAN-C 902. Another large advantage of the optical transducer is the absence of a thermal zero shift. Since the electrical components are thermally isolated, the zero shift due to temperature is eliminated. In many transducers, this error is as large as the thermal errors.

The response time to a step input can be approximated to be 0.5 mseconds, worst case. This is found by taking the response time of the filter and adding the delays due to the timing of the A/D circuit and the microprocessor. This is still an improvement over all of the transducers listed. The smaller diaphragm is primarily responsible for the decreased response time.

Overall, the optical transducer has excellent characteristics when compared to commercial transducers.

B Possible Refinements

While this initial study of the optical transducer is very promising, there are several refinements that could be incorporated to make the transducer even more attractive for industrial use. These refinements can be classified as diaphragm, optical, filter, and processor improvements.

1. Diaphragm Improvements

The diaphragm used throughout this study was chosen for some of it's properties that make it a good choice for transducer work. As seen in the temperature section, a better choice exists in steel diaphragms. By simply changing the design to incorporate the Ni-SPAN-C 902 diaphragm, the thermal sensitivity can be improved by a factor of over 35.

Another way to improve the transducer would be to use either a quartz or silicon diaphragm. The use of a crystalline structure virtually eliminates the effects of hysteresis and repeatability. Besides eliminating hysteresis, a quartz diaphragm will have much better thermal shift behavior. The quartz diaphragm used in the Setra 250 contains a quartz diaphragm that has 1/30 the thermal expansion and 1/100 the hysteresis of stainless steel[35].

2. Optical Improvements

Several possibilities exist for improving the optical circuit. One is to replace the seven fiber system with a bundle system packed with miniature fibers. The sensitivity will drastically increase, but the theoretical characteristic equation becomes more difficult to calculate, especially if the transmit and receive fibers are arranged randomly. For the optical transducer, the exact equation would not be important since the overall transducer equation is curve fit.

A laser could be used as the light source. This would greatly increase the intensity of the light transmitted, thereby improving the resolution of the received light.

It would also be possible to decrease or increase the fiber sizes along with the diaphragm size in order to optimize the natural frequency of the diaphragm. There are some physical limitations on how small the fibers and the diaphragm can be, but there is room for improvement in this area.

3. Filter Improvements

The filter circuit was introduced to help the transducer respond to fast transients. Other filter types could be employed to yield the same or better results with fewer stages of filtering. For example, a Chebyshev filter to meet the same specifications that the sixth order Butterworth filter meets would only have to be of order five.

The desired filtering could be carried out in the microprocessor. To accomplish this, a digital signal processor would be more appropriate than the 8086 system proposed in this study. The requirement would focus on the ability to do the sixth order fit as quickly as possible. A faster A/D Converter would be needed to allow the system to sample at a fast enough rate to filter effectively.

4. Processor Improvements

As just discussed, the incorporation of a digital signal processor that can support floating point arithmetic would greatly speed up the system, allowing for digital filtering and improving response time. A faster A/D Converter is easily incorporated, but not until the processor conversion time can be reduced below 45 μseconds.

Other possible improvements in the processor circuit would be a control system for the transducer. The output of the light source could be varied to increase the intensity of the received light at low levels. This would make the transducer attractive for large range measurements where greater accuracy is desired for smaller pressures.

C Summary

The optical transducer presented here has certain advantages over today's commercial transducers. While this study is not all inclusive, it does indicate that there is a real potential in using optical techniques such as this in industrial devices for pressure measurement. The reflective method offers significantly greater accuracy, a doubling of dynamic range, and reduced temperature dependence because of its isolated optics and electronics.

The next step in the design process would be the construction of a prototype transducer. This would allow the study of the behavior of the actual system and permit the theoretical design to be refined. As stated in the introduction, optical techniques are finding increased use in instrumentation. While standard pressure measurement techniques will continue to be used, optical techniques will undoubtedly find their way into industrial pressure measurement as improved optical and electronic technologies develop.

LIST OF REFERENCES

LIST OF REFERENCES

1. Jerry L. Lyons. The Designers Handbook of Pressure-Sensing Devices. St. Louis: Van Nostrand Reinhold Co., 1980. Page 147.

2. Kendall L. Belsley, David R. Huber, and Jack Goodman. All Passive Fiber Optic Pressure Sensor. Intech Magazine, Dec 1986. Pages 39-42.

3. Mario Di Giovanni. Flat and Corrugated Diaphragm Design Handbook. New York: Marcel Dekker Inc., 1982.

4. W. B. Allan. Fibre Optics; Theory and Practice. New York: Plenum Press, 1973. Page 80.

5. Mario Di Giovanni. Page 1.

6. Ibid. Page 14.

7. Ibid. Page 130.

8. Ibid. Page 148.

9. Ibid. Page 157.

10. Ibid. Page 130.

11. Ibid. Page 160.

12. Ibid. Page 158.

13. Gould Electronics Inc. Gould Electronics Catalog. Oxnard: Technical Bulletin TF0013.

14. Mario Di Giovanni. Page 194.

15. Ibid. Page 56.

16. W. B. Allan. Page 8.

17. Fiberguide Industries. 1987 Fiberguide Industries. Stirling: Product Catalog. Page 1.

18. T. C. Hsia. System Identification. Lexington: Lexington Books. Pages 22-25.

19. Fiberguide Industries. Page 3.

20. Hewlett Packard Inc. Optoelectronics Designer's

Catalog. Palo Alto: Hewlett Packard, 1987. Page 8-43.

21. Ibid. Page 8-49.

22. G. S. Moschytz and P. Horn. Active Filter Design Handbook. New York: John Wiley and Sons, 1981. Page 131.

23. Ibid. Page 134.

24. M. S. Ghausi and K. R. Laker. Modern Filter Design. Englewood Cliffs: Prentice Hall, 1981. Page 282.

25. Ibid. Page 180.

26. Ibid. Page 179.

27. Analog Devices. 1984 Databook; Volume I. Norwood: Analog Devices, 1984. Page 4-135.

28. Ibid. Page 10-23.

29. Ibid. Page 10-175.

30. Ibid. Page 10-111.

31. INTEL. Microsystems Component Handbook. Santa Clara: INTEL, 1986. Pages 3-1 and 3-219.

32. Texas Instruments. TMS32010 Users Guide. Dallas: Texas Instruments, 1987. Page 2-1.

33. Mario Di Giovanni. Page 127.

34. Ibid. Page 127.

35. Setra Systems. Setra Systems Bulletin AGP-201. Acton: Setra Systems Inc., 1982.

36. MKS. MKS Instruction Manual 195-109700-A-3/85. Burlington: MKS Instruments Inc., 1985.

37. Schaevitz Engineering. Schaevitz Technical Bulletin 3001A. Pennsauken: Schaevitz Engineering, 1984.

38. Schaevitz Engineering. Schaevitz Technical Bulletin 3103A. Pennsauken: Schaevitz Engineering, 1984.

39. W. B. Allan. Page 47.

APPENDIX

DERIVATION OF THE OPTICAL SENSOR CHARACTERISTIC EQUATION

A Ideal Equation

For use as a pressure transducer, the relationship between the distance d and the flux of the received light Φ_R must be known. First, the relationship between the distance d and the received flux Φ_R will be derived considering an ideal system, one where there is no flux lost throughout the system. Once the ideal equation has been derived, the losses will be taken into account to yield a more realistic equation.

With the assumption that no light is lost due to absorption or to scattering, the problem of determining the relationship becomes a geometric problem. Using the receiving fibers as a point of reference, the transmitted light irradiates a light spot that is a circle of radius r+2a by the time it reaches the fibers (Fig. 14). As d becomes larger, the circle of light "seen" at the receivers becomes larger. The amount of flux received is proportional to the area of the light spot that overlaps the receive fibers.

Due to the symmetry of the receivers, the derivation can be done with a two fiber system. The seven fiber system shown in Figure 5 would have the same characteristic equation multiplied by six.

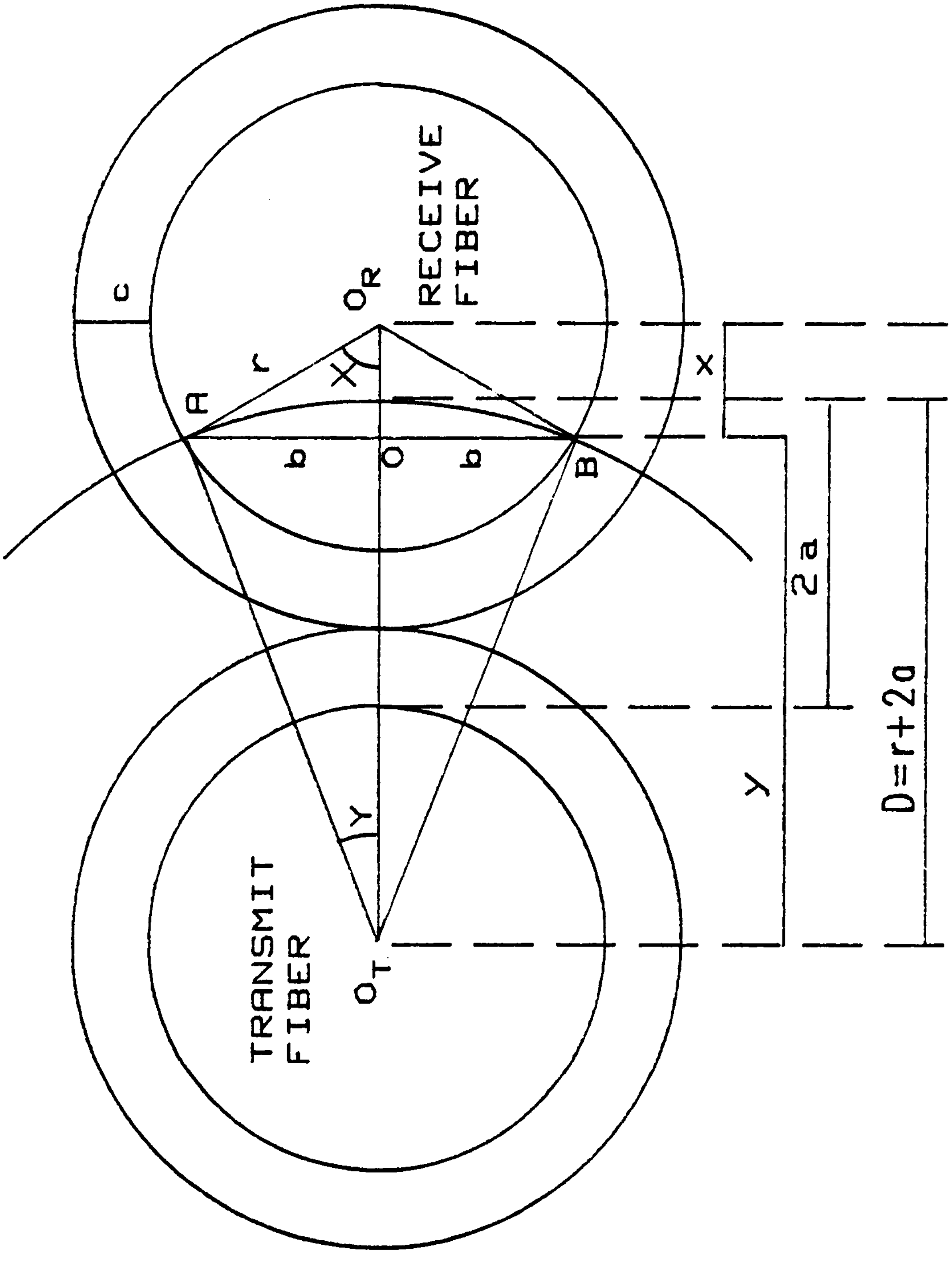

Figure 14: A Two Fiber System

Referring to Figure 14, the two fiber system has the following variables of interest:

1. r is the radius of the fiber cores (in.).
2. c is the thickness of the cladding (in.).
3. R is the total fiber radius, r+c (in.).
4. $\overline{AB}$ is the line segment that runs between the points of intersection of the two circles of radii r and D.
5. D is the radius of the light spot seen at the receiver. D=r+2a (in.).
6. 2a is the amount that the light spot has grown due to the distance d.
7. $\overline{O_TO_R}$ is the line segment that joins the centers of the two fibers.
8. O is the point of intersection between $\overline{AB}$ and $\overline{O_TO_R}$.
9. b is the distance between A and O as well as the distance between B and O.
10. x is the distance between O_R and O.
11. y is the distance between O_T and O.
12. X is the angle formed by $\overline{OO_R}$ and $\overline{AO_R}$.
13. Y is the angle formed by $\overline{OO_T}$ and $\overline{AO_T}$.

The areas of interest are:

1. The total area of the light spot of radius r+2a, A_T.

2. The area of the intersection of the receiver fiber core and the light spot, A.

The area of the light spot at the receiver is just

$$A_T = \pi(r+2a)^2$$

To get the area of the intersection, consider the intersection of the circles to be the sum of the areas formed by the common chord $\overline{AB}$, which has a length 2b. This area is just

$$A = Xr^2 + YD^2 - b(x+y) \qquad (A1)$$

where X, Y, b, x, and y are unknown.

Referring to Figure 14, the following relationships are known:

$$x + y = 2R = 2(r+c) \qquad (A2)$$

$$b^2 + x^2 = r^2 \qquad (A3)$$

$$b^2 + y^2 = D^2 = (r+2a)^2 \qquad (A4)$$

$$\cos(X) = x/r \qquad (A5)$$

$$\cos(Y) = y/D = y/(r+2a) \qquad (A6)$$

Since X and Y are defined in terms of x and y, there are only three unknowns. Solving for x, y, and b

$$y = \left[\frac{4R^2+D^2-r^2}{4R}\right] \qquad (A7)$$

$$x = 2R - y = \left[\frac{4R^2-D^2+r^2}{4R}\right] \qquad (A8)$$

and,

$$b = \left[\frac{[16r^2R^2-(4R^2-D^2+r^2)^2]^{1/2}}{4R}\right] \qquad (A9)$$

Therefore

$$X = \cos^{-1}\left[\frac{x}{r}\right] = \cos^{-1}\left[\frac{(4R^2-D^2+r^2)}{4Rr}\right] \qquad (A10)$$

and

$$Y = \cos^{-1}\left[\frac{y}{D}\right] = \cos^{-1}\left[\frac{(4R^2+D^2-r^2)}{4RD}\right] \qquad (A11)$$

These equations are valid for $(r+c) \le D \le 3R$. At $D=(3r+2c)$, the entire receive fiber is covered by the light spot.

Recalling the equation of the area of intersection;

$$A = Xr^2 + YD^2 - b(x+y) \qquad (A1)$$

and substituting the values for x, y, and b;

$$A = r^2\cos^{-1}[x/r] + D^2\cos^{-1}[y/D] - 2Rb \qquad (A12)$$

where x, y, and b have been derived as before.

Using the fact that $D=r+2a$ and $R=r+c$, the equation for the area of intersection becomes

$$A = r^2\cos^{-1}\left[\frac{x}{r}\right] + (r+2a)^2\cos^{-1}\left[\frac{y}{r+2a}\right] - 2(r+c)b \qquad (A13)$$

where

$$x = \left[\frac{(r+c)^2-(ar+a^2)}{r+c}\right] \qquad (A14)$$

$$y = \left[\frac{(r+c)^2+(ar+a^2)}{r+c}\right] \qquad (A15)$$

and

$$b = \left[\frac{[r^2(r+c)^2-\{(r+c)^2-(ar+a^2)\}^2]^{1/2}}{r+c}\right] \qquad (A16)$$

With the assumption that no flux is lost from transmit to receive, the flux received is just the percentage of the light spot that falls on the receive fiber times the flux of the transmitted light, Φ_T, or

$$\Phi_R = \Phi_T A/A_T \tag{A17}$$

where A is defined above.

The expression for Φ_R is

$$\Phi_R = \Phi_T A/A_T = \Phi_T\left[\frac{Xr^2+YD^2-b(x+y)}{\pi D^2}\right] \tag{A18}$$

where X, Y, x, y, and b are defined above.

By using six receive fibers as in Figure 5, the sensitivity of the sensor is increased by six and,

$$\Phi_R = 6\Phi_T A/A_T \tag{A19}$$

This equation is valid for $(r+2c) \leq D \leq (3r+2c)$. Since $D=(r+2a)$, the equation is valid for $c \leq a \leq (r+c)$. For $0 \leq a \leq c$, there is no light picked up at the receive fibers and for $a \geq (r+c)$, the receiver areas are covered by light, and the only thing that changes is the area of the light spot.

The entire function for the received light is:

1) $\Phi_R = 0$ for $0 \leq a \leq c$

2) $\Phi_R = \Phi_T 6\left[\frac{[Xr^2+YD^2-2b(r+c)]}{\pi D^2}\right]$ for $c \leq a \leq r+c$

3) $\Phi_R = (\Phi_T 6r^2)/D^2$ for $a \geq r+c$

In order to simplify the equations, consider the case where $c=0.10r$. This is a typical value of the cladding thickness for fibers[17]. Also, let Ω be defined as the ratio of received light to transmitted light($\Omega=\Omega_R/\Omega_T$). Using c=0.10r, Ω becomes

$$\Omega = 6\left[\frac{Xr^2+YD^2-b(x+y)}{\pi D^2}\right] \tag{A20}$$

where X, Y, and b are defined in equations A9, A10, and A11. Recalling that x+y = 2(r+c), the entire function for Ω can be written as

$$\Omega = 0 \qquad \text{for } 0\le a\le 0.10r$$

$$\Omega=6\left[\frac{r^2\cos^{-1}\left[\dfrac{1.21r^2-(ar+a^2)}{1.10r^2}\right]+(r+2a)^2\cos^{-1}\left[\dfrac{1.21r^2+(ar+a^2)}{1.10r^2+2.20ar}\right]}{\pi(r+2a)^2}\right]$$

$$- 6\left[\frac{2[1.21r^4-\{1.21r^2-(ar+a^2)\}^2]^{1/2}}{\pi(r+2a)^2}\right] \tag{A21}$$

$$\text{for } 0.10r\le a\le 1.10r$$

$$\Omega = \left[\frac{6r^2}{(r+2a)^2}\right] \qquad \text{for } a\ge 1.10r \tag{A22}$$

B Losses in the System

The optical receiver can experience losses at the following locations:

1. The coupling out of the source into the transmit fiber.
2. The transmit fiber.
3. The fiber/air junction from the transmit

fiber to the diaphragm surface.

4. The diaphragm surface.
5. The air/fiber junction into the receive fiber.
6. The receive fiber.
7. The coupling into the receiver from the receive fibers.

Losses in fiber optic systems can be classified as follows[39]:

1. Fresnel Reflection losses.
2. Absorption losses.
3. Interface losses.
4. Fiber Transmission losses.

Absorption losses are related to imperfections within the core material and are usually measured in dB/km. For the length of fiber being used in the receiver, the absorption loss is insignificant. Interface losses are losses that occur at the core/cladding interface due to imperfections in manufacturing. These losses are insignificant due to the short length of fiber used and the quality of fibers being produced today. Fiber transmission losses are related to the distance of the fiber being used and the Numerical Aperture of the fiber. Every time a ray is internally reflected at the cladding, some minute amount of flux is lost. For the optical receiver, this loss can be ignored as well.

The losses due to the coupling at the source and the receiver can be ignored. Typically, any air gap that may exist between the fibers and the optical devices will be filled with an index matching epoxy to minimize losses in the junction.

The losses due to Fresnel Reflection cannot be ignored because of their magnitudes. Fresnel losses occur at fiber/air junctions because of the difference in indices of refraction between air and the fiber. Some of the light that hits a fiber/air junction will be internally reflected. If the fraction of light that is reflected at a fiber/air junction is defined as A_f, then

$$A_f = \left[\frac{(n_1-n_0)^2}{(n_1+n_0)^2}\right] \tag{A23}$$

where

n_1 is the index of refraction of the fiber.

n_0 is the index of refraction of the air.

For purposes of this study, consider a fiber with a silica core that has an index of refraction of n_1=1.620. The index of refraction of the air is n_0=1.000. The amount of light reflected at a fiber/air junction will be

$$A_f = 0.0560 \tag{A24}$$

This means that at every air/fiber junction, 5.6% of the light will be internally reflected.

There are two such surfaces in the receive circuit. There is an air/fiber junction between the transmit fiber and the diaphragm and between the diaphragm and the receive fibers. At the transmit fiber junction, assume that 100% of the produced light flux arrives. According to equation A23, 94.6% will pass through that junction and irradiate the diaphragm surface. Assuming a perfectly reflective surface, 94.6% of the original light flux will now hit the receive fibers. Of this 94.6%, only 94.6% will pass through the junction, or 89.49% of the original flux. From this simple scenario, it is shown that more than 10% of the light flux produced at the source is not available to the detector. While this is a significant amount, it is not that critical to the operation of the receive circuit. Of greater importance to the designer is the repeatability of the optical receiver circuit. Optical products are extremely reliable and repeatable. Once the losses have been taken into account, there will be no fluctuation in system losses.

The only otheer is the loss at the diaphragm surface. The diaphragm rigid center needs to have a highly polished and reflective surface. If the surface is not reflective enough, a thin reflective film can be applied which will give the surface a reflectivity very close to one. Again, it's not important that the reflectivity be one, only that the reflectivity be constant so the receiver repeatability is maintained.

For purposes of this study, only Fresnel losses will be considered. As was shown earlier, with a fiber core made of silica, the losses due to the Fresnel reflections will be about 11.51%. This factor will decrease the overall equation for Ω to

$$\Omega = 0 \qquad \text{for } 0 \le a \le 0.10r$$

$$\Omega=5.3694\left[\frac{r^2\cos^{-1}\left[\dfrac{1.21r^2-(ar+a^2)}{1.10r^2}\right]}{\pi(r+2a)^2}\right]$$

$$+\ 5.3694\left[\frac{(r+2a)^2\cos^{-1}\left[\dfrac{1.21r^2+(ar+a^2)}{1.10r^2+2.20ar}\right]}{\pi(r+2a)^2}\right]$$

$$-\ 5.3694\left[\frac{2[1.21r^4-\{1.21r^2-(ar+a^2)\}^2]^{1/2}}{\pi(r+2a)^2}\right] \qquad \text{(A25)}$$

$$\text{for } 0.10r \le a \le 1.10r$$

$$\Omega = \left[\frac{5.3694r^2}{(r+2a)^2}\right] \qquad \text{for } a \ge 1.10r \qquad \text{(A26)}$$

To normalize Equations A25 and A26, they are expressed in terms of

$$z \equiv a/r$$

so that

$$\Omega = 0 \qquad \text{for } 0 \le z \le 0.10$$

$$\Omega=5.3694\left[\frac{\cos^{-1}\left[\dfrac{1.21-(z+z^2)}{1.10}\right]+(1+2z)^2\cos^{-1}\left[\dfrac{1.21+(z+z^2)}{1.10+2.20z}\right]}{\pi(1+2z)^2}\right]$$

$$- 5.3694\left[\frac{2[1.21-\{1.21-(z+z^2)\}^2]^{1/2}}{\pi(1+2z)^2}\right] \qquad \text{(A27)}$$

$$\text{for } 0.10 \le z \le 1.10$$

$$\Omega = \left[\frac{5.3694}{(1+2z)^2}\right] \qquad \text{for } z \ge 1.10 \qquad \text{(A28)}$$

Table 2 shows the values of Ω for z between 0 and 2.00; Figure 15 is a plot of Ω vs. z. Of particular interest to the designer is the front slope of the curve, particularly where the slope is greatest. Figure 16 and Table 3 show the values of Ω for z between 0.10 and 0.50, where Ω is most sensitive to changes in z.

TABLE 2

Values of the function Ω as z varies from 0 to 2.00

z	$\Omega(z)$	z	$\Omega(z)$	z	$\Omega(z)$
0.00	0.00000	0.43	0.38145	0.84	0.56991
		0.44	0.39037	0.86	0.57109
0.10	0.00000	0.45	0.39904	0.88	*0.57160
0.11	0.00453	0.46	0.40746	0.90	0.57143
0.12	0.01244	0.47	0.41563	0.92	0.57056
0.13	0.02218	0.48	0.42357	0.94	0.56899
0.14	0.03316	0.49	0.43126	0.96	0.56670
0.15	0.04501	0.50	0.43872	0.98	0.56365
0.16	0.05750	0.51	0.44595	1.00	0.55981
0.17	0.07044	0.52	0.45294	1.02	0.55511
0.18	0.08370	0.53	0.45970	1.04	0.54946
0.19	0.09715	0.54	0.46624	1.06	0.54273
0.20	0.11073	0.55	0.47256	1.08	0.53463
0.21	0.12436	0.56	0.47866	1.10	0.52436
0.22	0.13798	0.57	0.48454		
0.23	0.15155	0.58	0.49020	1.15	0.49306
0.24	0.16502	0.59	0.49566	1.20	0.46448
0.25	0.17838	0.60	0.50090	1.25	0.43832
0.26	0.19157	0.61	0.50594	1.30	0.41431
0.27	0.20460	0.62	0.51078	1.35	0.39221
0.28	0.21743	0.63	0.51542	1.40	0.37184
0.29	0.23006	0.64	0.51985	1.45	0.35302
0.30	0.24247	0.65	0.52409	1.50	0.33559
0.31	0.25466	0.66	0.52814	1.55	0.31942
0.32	0.26660	0.67	0.53199	1.60	0.30439
0.33	0.27831	0.68	0.53566	1.65	0.29039
0.34	0.28971	0.69	0.53913	1.70	0.27735
0.35	0.30097	0.70	0.54243	1.75	0.26516
0.36	0.31193			1.80	0.25375
0.37	0.32263	0.72	0.54846	1.85	0.24307
0.38	0.33307	0.74	0.55378	1.90	0.23305
0.39	0.34326	0.76	0.55838	1.95	0.22363
0.40	0.35319	0.78	0.56229	2.00	0.21478
0.41	0.36286	0.80	0.56551		
0.42	0.37228	0.82	0.57109		

* Ω_{max} occurs at $z \approx 0.88$.

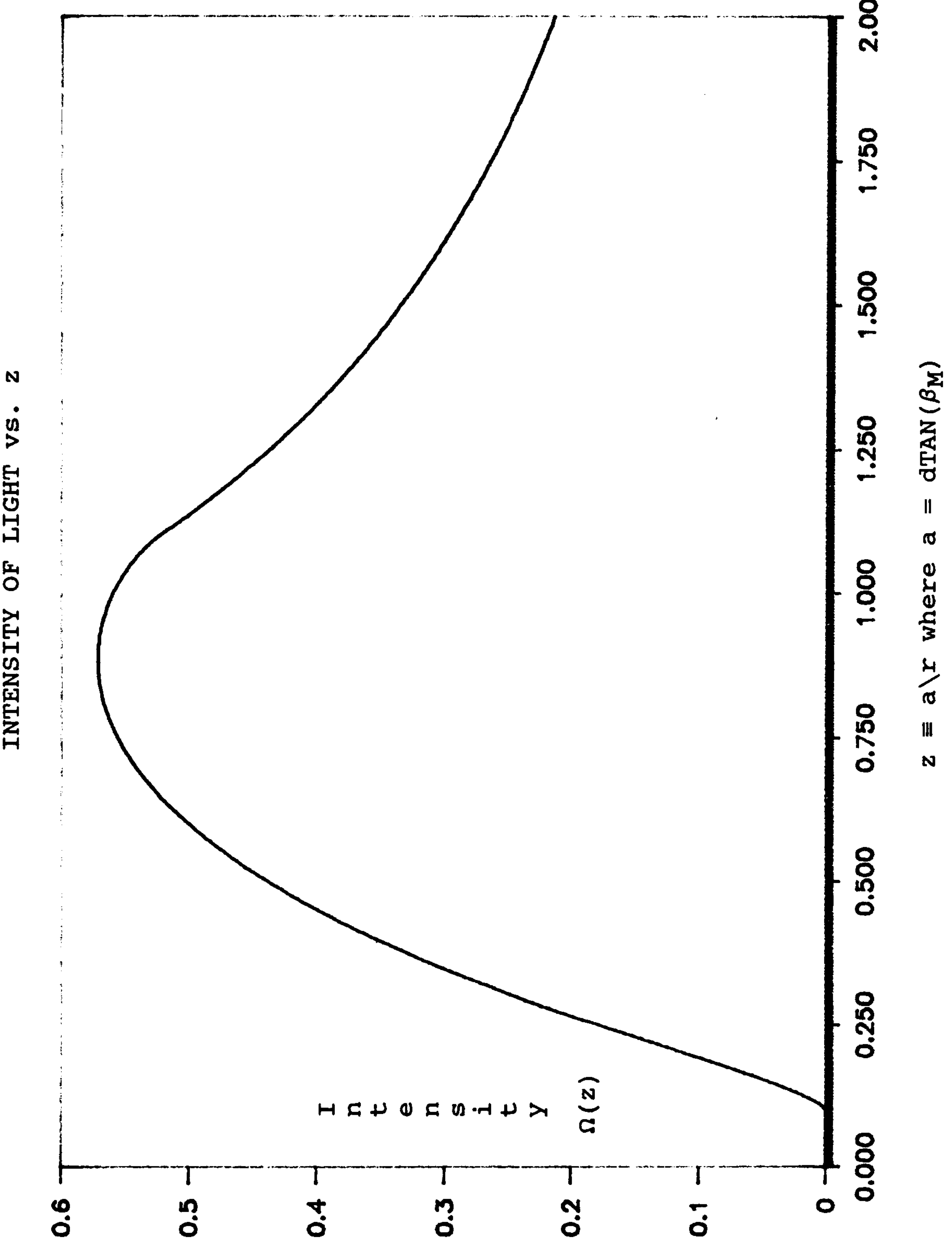

Figure 15: The Function Ω(z)

TABLE 3

Values of the function Ω as z varies from 0.10 to 0.50

$$\Omega(z)=5.3694\left[\frac{\cos^{-1}\left[\frac{1.21-(z+z^2)}{1.10}\right]+(1+2z)^2\cos^{-1}\left[\frac{1.21+(1+z^2)}{1.10+2.20z}\right]}{\pi(1+2z)^2}\right]$$

$$-\ 5.3694\left[\frac{2[1.21-[1.21-(z+z^2)]^2]^{1/2}}{\pi(1+2z)^2}\right]$$

z	Ω(z)	z	Ω(z)	z	Ω(z)
0.100	0.00000	0.240	0.16502	0.380	0.33307
0.105	0.00163	0.245	0.17172	0.385	0.33832
0.110	0.00453	0.250	0.17838	0.390	0.34326
0.115	0.00820	0.255	0.18499	0.395	0.34825
0.120	0.01244	0.260	0.19157	0.400	0.35319
0.125	0.01713	0.265	0.19811	0.405	0.35806
0.130	0.02218	0.270	0.20460	0.410	0.36286
0.135	0.02754	0.275	0.21104	0.415	0.36760
0.140	0.03316	0.280	0.21743	0.420	0.37228
0.145	0.03900	0.285	0.22378	0.425	0.37772
0.150	0.04501	0.290	0.23006	0.430	0.38145
0.155	0.05120	0.295	0.23630	0.435	0.38594
0.160	0.05750	0.300	0.24247	0.440	0.39037
0.165	0.06393	0.305	0.24859	0.445	0.39473
0.170	0.07044	0.310	0.25466	0.450	0.39904
0.175	0.07704	0.315	0.26066	0.455	0.40328
0.180	0.08370	0.320	0.26660	0.460	0.40746
0.185	0.09041	0.325	0.27249	0.465	0.41157
0.190	0.09715	0.330	0.27831	0.470	0.41563
0.195	0.10394	0.335	0.28407	0.475	0.41963
0.200	0.11073	0.340	0.28971	0.480	0.42357
0.205	0.11755	0.345	0.29540	0.485	0.42744
0.210	0.12436	0.350	0.30097	0.490	0.43126
0.215	0.13118	0.355	0.30648	0.495	0.43502
0.220	0.13798	0.360	0.31193	0.500	0.43872
0.225	0.15155	0.365	0.31731		
0.230	0.15155	0.370	0.32263		

The region of $\Omega(z)$ from z=0.10 to 0.50 has the greatest sensitivity (i.e. the greatest slope, $d\Omega/dz$)

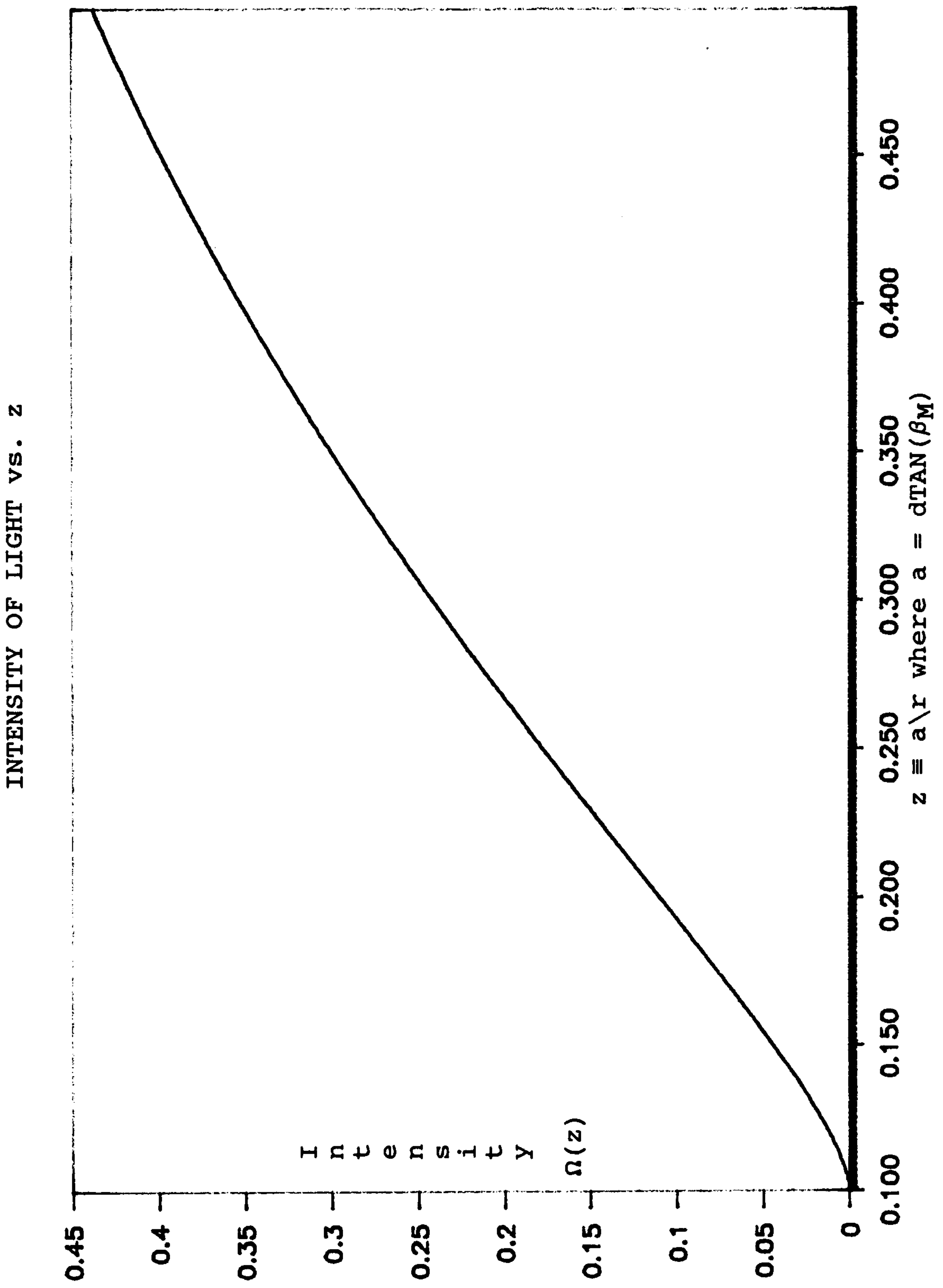

Figure 16: The Function $\Omega(z)$ in the Useful Range of z

VITA

William Bruce DeShetler was born in Toledo, Ohio on June 6, 1957. He attended elementary and high school in Toledo and graduated from Morrison R. Waite High School in June 1975. He attended the University of Toledo on a part time basis until he entered the United States Air Force in 1980. He was first stationed at Chanute Air Force Base in central Illinois. While at Chanute, he was awarded his Associates Degree in Electronic Systems Technology from the Community College of the Air Force.

In 1983, he went to the University of Illinois in Champaign where he received a Bachelor of Science in Electrical Engineering and graduated in June 1985 with Highest Honors.

After graduating from Illinois, he was stationed at Arnold Air Force Base in Tennessee. He entered the Graduate School of The University of Tennessee in 1985 and completed the requirements for a Masters of Science degree with a major in Electrical Engineering in August 1988.

The author is currently employed in the United States Air Force at Arnold Air Force Base, Tennessee.